

## Final Report

### **Integrated Accelerated Precipitation Softening (APS) – Microfiltration (MF) Assembly and Process Development to Maximize Water Recovery during Energy Production and CO<sub>2</sub> Sequestration**

PI: Jonathan A. Brant, Assistant Professor, Department of Civil and Architectural Engineering,  
University of Wyoming,

Co-PI: Dongmei (Katie) Li, Assistant Professor, Department of Chemical and Petroleum  
Engineering, University of Wyoming

Project Duration: 03/01/2012 to 02/28/2014

**Abstract:** The development of Wyoming's energy resources (coal bed methane extraction [CBM], hydraulic fracturing) and carbon dioxide (CO<sub>2</sub>) sequestration sites all invariably result in the production of brackish wastewaters. The treatability of these waters varies from relatively simple for CBM water (dissolved solids < 2,000 mg/L) to complex for the water that is displaced during geologic sequestration of CO<sub>2</sub> (dissolved solids > 20,000 mg/L). Reverse osmosis (RO) is a proven desalination process, which requires hydraulic pressures to transport water across semi-permeable membranes. Although RO has been extensively used to treat a variety of source waters, including energy development produced water, managing the concentrate that is produced as a byproduct during RO has persisted as an environmental and economic challenge in maximizing water recovery rate. Here we propose to develop an integrated accelerated precipitation softening (APS)-microfiltration (MF) assembly for reducing the volume of concentrate that must be disposed of when using RO to treat high-salinity, energy activity related waters in Wyoming. The ability of chemical precipitation processes, including APS, to remove scale-forming elements from source waters is established. Conventional softening processes are hindered by the production of fine suspensions of mineral precipitates that require relatively long sedimentation times (1.5-3 hrs) and a residual sludge having a low solids content (2-30%). These issues generate concerns related to the size of softening facilities, solids carry over to downstream membrane processes, and sludge disposal. These concerns hinder the use of APS as a management strategy for RO concentrate. APS processes use calcite crystals to provide a preferential surface area for nucleation and growth to occur, thus accelerating the kinetics of mineral precipitation. As such, the accelerated APS process will allow the removal of CaCO<sub>3</sub> as well as other scale forming elements that will be incorporated in the CaCO<sub>3</sub> crystals and removed. Built upon the previous findings in the field of treating challenging source waters, the unique contribution of the proposed work lies in the three folds: 1) incorporating MF as a polishing step following precipitation softening and prior to secondary RO process; 2) application of calcite seeds to accelerate the softening process and to improve the treatability of the feed water for the secondary RO system; 3) application of an integrated rather than singular approach for maximizing the recovery/reuse potential of highly saline produced waters. The integrated APS-MF assembly for RO concentrate treatment will provide a superior feed water quality to secondary RO systems that will allow for water recovery ratios to approach, or exceed, 90%.

## INTRODUCTION

The development of energy resources and CO<sub>2</sub> sequestration sites results in production of a large amount of brackish wastewater. Fourteen to eighteen billion barrels of wastewater is produced per year in the United States from oil and gas drilling <sup>1</sup>. A high total dissolved solids (TDS) concentration is one of the aspects that make produced water difficult to manage. TDS concentrations range between 1,000 mg/L and 300,000 mg/L <sup>2</sup>. To put this in perspective, the Colorado River has a TDS concentration of 600-800 mg/L and seawater has a TDS concentration of 30,000 mg/L<sup>3</sup>. Water with a high TDS concentration will harm the environment if it is discharged to the soil surface, therefore it must be treated for re-use by desalination, or disposed of by re-injection or evaporation<sup>4-6</sup>. A conceptual decision tree for managing produced waters is given in **Figure 1**.

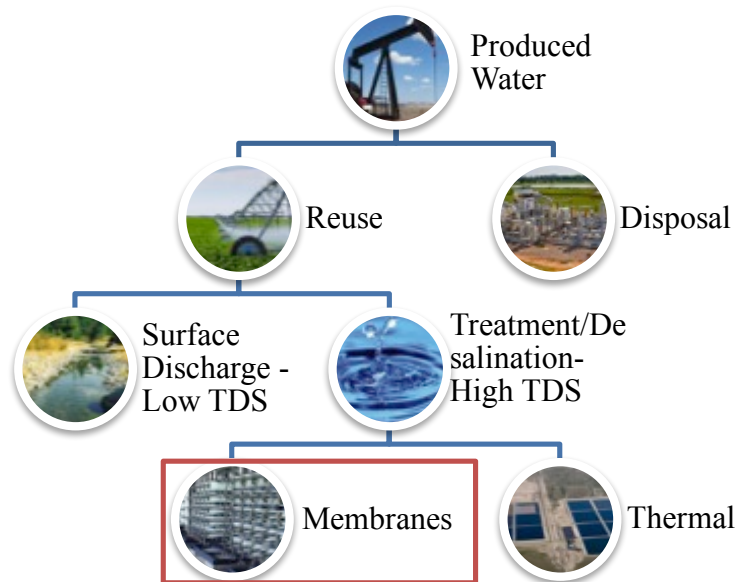


**Figure 1:** Schematic depicting current produced water disposal options. The red box indicates the category that this research falls within.

In **Figure 1**, the two common treatment strategies for desalination of produced water are membrane processes and thermal processes or distillation <sup>7,8</sup>. The advantages of membrane processes over thermal ones are that they typically require less energy to achieve separation <sup>9</sup>. However, membrane processes are characterized by lower overall water recoveries, or the amount of water that is converted into a product stream, compared to thermal processes. This is particularly evident for highly saline produced waters. For membrane processes the achievable water recovery is limited by many factors including membrane fouling, mineral precipitation (scale formation on the membrane), and the osmotic pressure that must be overcome to initiate water transport across the membrane. Low water recoveries are problematic for any number of reasons. Of most concern in this project was minimizing the volume of the concentrated reject stream that results from membrane desalination <sup>4</sup>.

Beneficial reuse of produced waters is of interest to the energy industry and other stakeholders because of the anticipated economic impacts for producers and reduction in the industry's water footprint <sup>1,10</sup>. This latter area is of particular importance to arid regions like Wyoming. Because

the TDS concentration found in produced water is in most cases higher than acceptable levels for potable and non-potable reuse applications some form of treatment is required. The development of a treatment protocol is essential to the success of on-shore oil and gas production due to economic and environmental concerns. Currently, reinjection of produced waters into subsurface formations range in cost from \$0.40 to \$1.75/bbl and installation of an injection well can cost up to \$3 million<sup>12</sup>. For comparison, seawater (TDS ~ 36,000 mg/L) reverse osmosis (RO) desalination systems are characterized by operating costs of approximately \$0.16/bbl and capital costs of \$125 to \$295/bpd<sup>12</sup>. It is difficult to compare the two options in general terms, however, it is clear that both options are economically burdensome to the producer. As population expands and access to fresh water is further limited, the economic viability of reverse osmosis as a reuse technology will increase<sup>1</sup>. A U.S. Department of Energy (DOE) report on hydraulic fracturing flow back water treatment identified a price target of  $\leq$  \$2/bbl<sup>13</sup>. Withstanding practical limitations RO was found meet this cost criteria; however, the presence of sparingly soluble metals and minerals presented a challenge to the application of RO because of fouling concerns<sup>13</sup>.

RO is a proven desalination technology that has been used for managing oil and gas produced waters<sup>13</sup>. Without proper pretreatment, RO systems treating produced waters have failed or performed poorly<sup>6,15,16</sup>, due to severe membrane fouling. In these application the most problematic type of membrane fouling has been mineral scaling in most cases. Common mineral scale forming elements include calcium, barium, magnesium, iron and strontium<sup>17-20</sup>. These elements precipitate onto the RO membrane once their supersaturation concentration is exceeded. Increasing the feasibility of RO treatment of produced waters requires that effective technologies be developed and implemented for removing scale forming elements so as to increase the water recovery during desalination<sup>4,21,22</sup>.

This overall goal of this work was to evaluate the effectiveness of accelerated precipitation softening (APS) combined with ceramic microfiltration (MF) membranes for removing scale forming elements from produced water. APS has been shown to reduce the concentration of scale forming elements, particularly calcium<sup>17,25-27</sup>, in complex source waters. Additionally, ceramic MF has been shown to effectively remove suspended solids from produced waters<sup>1,28,29</sup> while operating under high solids loading rates. A DOE report on cost, performance and mobility challenges for these two pretreatment steps found that lime softening meets the cost requirements but has performance challenges when silica is present and the treatment has low mobility<sup>13</sup>. Lime softening can be used for suspended solids, calcium, silica, and oil removal<sup>13</sup>. It was also reported here that MF is effective at removing suspended solids and oil at low cost with good mobility, but small particles create a performance challenge<sup>13</sup>. Integration of the two technologies, particularly while using ceramic rather than polymeric membranes, is expected to mitigate the inherent drawbacks associated with the individual processes

The overall objective of this project is to build and evaluate the performance of an integrated APS-MF process in order to dramatically improve the treatability of concentrate streams, thus increasing the overall water recovery rate for RO desalination systems. The specific tasks that were pursued in this work were as follows:

1. To what extent does calcium carbonate seeding improve reaction kinetics in precipitation softening of produced water?

2. What role does microfiltration play in the removal of dissolved and particulate forms of calcium following accelerated precipitation softening?
3. How does APS-MF treatment change the mineral fouling and the specific water flux for secondary RO treating produced water?

## EXPERIMENTAL

**Produced Water.** A synthetic water was created by dissolving dry inorganic salts, at the concentrations listed in **Table 1**, in doubly deionized water (DDW). The composition of the water was set to represent an average primary RO (PRO) concentrate, based on a survey of produced water chemistries in Wyoming

**Table 1:** Composition of synthetic PRO concentrate based on the average produced water quality found in Wyoming.

| Salt                            | Concentration |      |
|---------------------------------|---------------|------|
|                                 | mol/L         | g/L  |
| CaCl <sub>2</sub>               | 0.02          | 2.93 |
| Na <sub>2</sub> SO <sub>4</sub> | 0.04          | 5.05 |
| NaHCO <sub>3</sub>              | 0.02          | 1.72 |
| NaCl                            | 0.10          | 5.90 |

The dry salts purchased from Fisher Scientific (Waltham, MA) were sodium bicarbonate (powder, certified ACS) and sodium chloride (crystalline, certified ACS). calcium chloride dehydrate (ACS reagent), sodium sulfate anhydrous, while calcium carbonate powder (precipitated, heavy) were purchased from ACROS Organics (New Jersey, USA). Confocal microscopy of the calcium carbonate particles revealed an average particle size of 7.8 microns. Other research groups have shown this particle size of calcium carbonate to have a specific surface area of 0.8 m<sup>2</sup>/g<sup>56</sup>. Sodium hydroxide (10N, Fisher Scientific, Waltham, MA) was used for pH adjustment. Sulfuric acid (1N, VWR Scientific, Tualatin, OR) was used for acidification of reverse osmosis feed solutions.

**Optimization of Calcium Removal using APS.** A jar tester (Model 7790-711, Phipps & Bird, Richmond, VA) consisting of six three-liter plastic rectangular vessels with stir rods in each was used for initial precipitation experiments. The precipitation reaction was initiated by slowly adding sodium hydroxide to the synthetic PRO concentrate until the desired pH was achieved. Calcium carbonate particles were dispersed in the solution prior to pH adjustment in seeded experiments. The solutions were mixed at a speed of 45 RPM. Grab samples were taken from the jar tester using a 10 ml syringe, filtered using a 0.45-micron PVDF syringe filter (Millipore Corp., San Jose, CA), and analyzed to determine the dissolved calcium concentration. A range of pH values were explored, specifically 7.9, 9.5, 10.5, and 11.6. These values were chosen because they cover a range of saturation indices for calcium carbonate. These pH values correspond with Stiff and Davis Index values of 1.32, 3.06, 3.65, and 4.43, respectively. A dead-end filtration test cell apparatus (**Figure 2**) was used for both initial calcium removal studies via MF and preliminary RO membrane performance testing. Both MF and RO membranes used in the dead-end experiments were purchased from Sterlitech Corporation (Kent, WA).

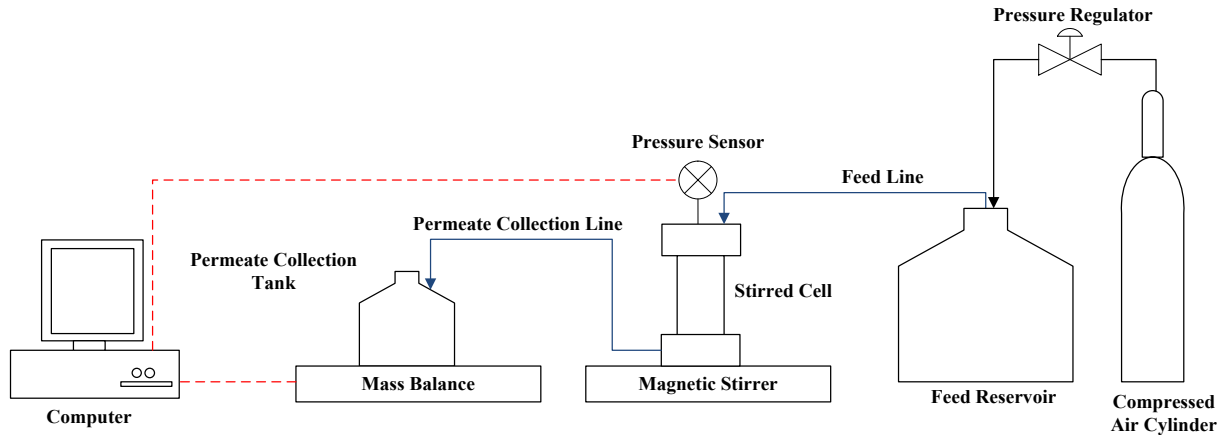


**Figure 2:** Process flow diagram of the dead-end membrane filtration/desalination test unit.

The feed solution was added to the 300 ml stirred cell assembly and the membrane disc was placed at the bottom of the cell. The active filter area for all dead-end filtration or permeation experiments was  $0.0015 \text{ m}^2$ . Air pressure was applied to the top of the cell until the desired operating pressure within the cell was reached. The microfiltration tests were performed at low pressure (2.0 bar) and run until all the feed solution was filtered through the membrane. The reverse osmosis tests were performed at high pressure (53 bar) and run for 12 hours. Filtrate was collected and weighed every 10 seconds (Model XS6035, Mettler Toledo, Columbus, OH). The experimental conditions and physical properties of the MF and RO membranes are listed in **Table 2**.

**Table 2:** Dead-end Experimental Conditions and Membrane Properties.

| Membrane  | Material | Pore Size   | Pure Water Specific Flux<br>$\text{L/m}^2 \text{ hr bar}$<br>20 °C | pH Range | Operating Pressure (bar) | Stirring Speed (RPM) |
|-----------|----------|-------------|--|----------|--------------------------|----------------------|
| PES MF    | PES      | 0.45 micron | 647  | 2-12     | 2.0                      | 150                  |
| DOW SW RO | PA       | MWCO 100 D  | 0.04   | 2-11     | 53                       | 300                  |

Calcium removal by, and fouling of the, MF were assessed using three types of feed water, *i.e.*, untreated, no-seeds, and APS. The untreated feed refers to the synthetic PRO concentrate with no treatment or pH adjustment. To initiate precipitation, the no-seeds feed sample was created by adjusting the pH of the synthetic PRO concentrate to 10.5 using sodium hydroxide (NaOH) and constantly stirring at 45 RPM for 10 minutes. Subsequently, the entire reaction content was poured into the stirred cell. For samples referred to as APS, 7 g/L of calcium carbonate seeds were added to the synthetic PRO concentrate, in addition to adjusting their pH to 10.5. The seeded APS water sample with pH 10.5 was then stirred continuously at 45 RPM for 10 minutes and poured into the stirred cell. Grab samples were taken, using a 10 ml syringe, from the starting feed water, as well as the filtrate, for water quality analysis, including turbidity and calcium concentration. Fouling of the RO membranes was assessed using two different feed solutions. The first solution is the untreated discussed above, while the second being the above APS solution followed by

microfiltration treatment, which is thereby referred to as ‘APS+MF’ sample. In order to minimize the occurrence of calcium carbonate membrane fouling, the pH of both feed solutions was reduced to pH 5.5 using sulfuric acid to dissolve remaining calcium carbonate precipitate.

***Integrated APS-MF System Performance Analysis.*** APS experiments were done in a 5 L jacketed glass reactor (Prism Research, Raleigh, NC) with a conical bottom. A constant temperature of 20 °C was maintained using a recirculating digital temperature bath (Model Isotemp 3028P, Fisher Scientific, Waltham, MA). A constant mixing speed of 45 RPM was maintained using a three-blade mixer. First, 7 g/L of calcium carbonate seeds were added to the synthetic PRO concentrate (**Table 1**). After adding the seeds, the APS reaction was initiated by slow addition of sodium hydroxide until pH 10.5 was achieved. The reaction was allowed to proceed until a stable calcium concentration was achieved. Following the APS treatment, the contents of the reactor were pumped from the bottom of the reactor to the cross-flow microfiltration module. Mixing continued in the feed reactor at 45 RPM throughout the microfiltration treatment.

Ceramic MF membranes were selected for this phase of the APS-MF study because of their high chemical stability, durability, and water flux and, most importantly, wide pH tolerance (2-13). Specifically, a titanium dioxide membrane with a nominal pore size of 0.45 µm was purchased from Sterlitech Corporation (Kent, WA), which was constructed as a 250 mm long tube with 7 tubular channels, each having the diameter of 2 mm. The module was operated in an inside-out flow configuration, where feed solution was introduced to the inside of the channels. The membrane was housed in a stainless steel tube from Sterlitech Corporation (Kent, WA) that allowed for continuous cross-flow operation. The pure water specific flux for the membrane at 20°C was determined to be 37 L/m<sup>2</sup> hr bar.

The feed solution was pumped into the cross-flow ceramic microfiltration module (Sterlitech Corporation, Kent, WA) through a flow meter (Model 104FloSen, McMillian CO, Georgetown, Texas) by the feed pump (Model 7523-80, Cole Parmer, Vernon Hills, IL), following the blue line. Backpressure was applied to the module by restricting flow of concentrate returning to the feed reactor. The concentrate flow was controlled using a diaphragm liquid backpressure valve (Model EB2NL2, Equilibar, Fletcher, NC), which was opened and closed using regulated air pressure on the diaphragm. Pressure increase across the microfiltration module resulted in an increase of filtrate across the microfiltration membrane. The filtrate then passed through a flow meter (Model L-50CCMD, Cole Parmer, Vernon Hills, IL) before being collected. Pressure transducers (Setra, Boxborough, MA) were mounted on both the filtrate and concentrate lines exiting the module. The APS-MF system was operated in two different modes: filtrate withdraw and filtrate recycle. In the filtrate withdraw mode the filtrate was collected in a storage vessel. In this mode, the concentration of those materials in the feed solution that were rejected by the MF membrane increased over time. In the filtrate recycle mode the system was operated as a closed loop system. Therefore, the concentrations of materials in the feed solution remained relatively constant over time.

Grab samples for water quality analysis of the starting PRO concentrate, APS effluent, and filtrate after MF treatment were collected. The calcium concentration, turbidity, and total suspended and dissolved solids of each solution were determined for each sample. Decline in TMP or filtrate flux during filtration is often used indicators for membrane fouling. For the APS-MF system, the filtrate flux was set as a constant, while the TMP was measured to monitor changes in membrane resistance, which is proportional to membrane fouling.

## RESULTS AND DISCUSSION

**Optimization of Calcium Removal in APS.** The solution chemistry and reaction conditions for removing calcium through precipitation and APS are well-established in the literature<sup>25-27,30,39,48</sup>. Maximizing calcium removal, while mitigating fouling of downstream MF membranes in the APS treatment scheme, remains however less understood, especially when the untreated water has high TDS concentrations, such as produced waters. The fouling propensity of the untreated PRO concentrate (**Table 1**) and APS treated produced water samples with TDS of 14,000 mg/L were therefore assessed for the MF membranes, while measuring calcium removal. Specific process variables that were optimized during these tests included solution pH, calcium carbonate seed concentration, and reaction time within the softening reactor. Optimal reaction conditions were defined as those that resulted in the most rapid reaction (precipitation) kinetics and the greatest amount of calcium removal. Calcium removal as a function of solution pH is reported in **Figure 3** for the produced water sample represented in **Table 1**. As demonstrated in **Figure 3a** calcium removal increased as the solution pH became more basic in accordance with established calcium solubility relationships.

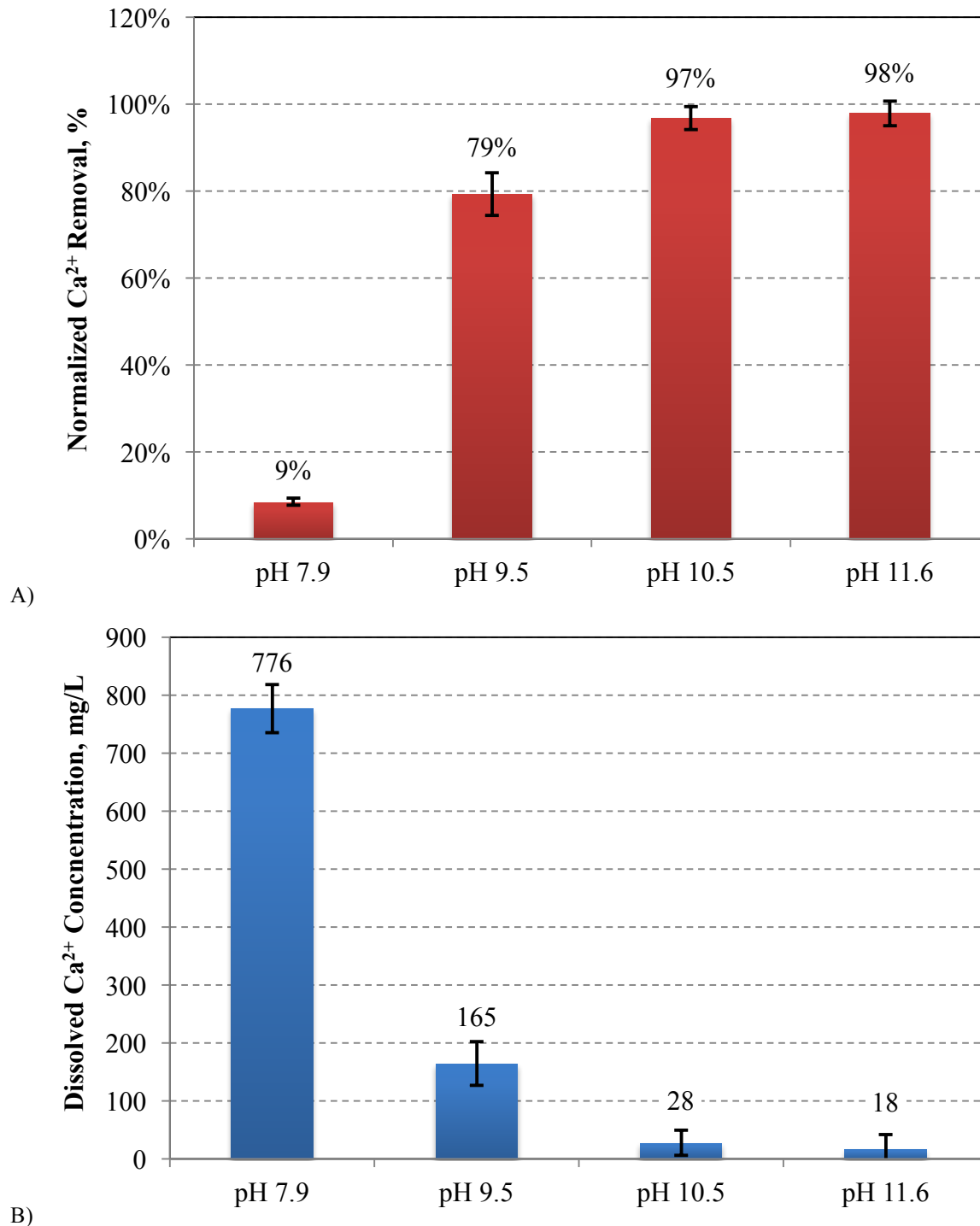


**Figure 3:** Calcium reduction via jar precipitation softening for various pH conditions after 1 hour of reaction and 45 RPM stirring speed. (A) Percent reduction in calcium reduction (B) Final dissolved calcium concentration after softening (# of samples per pH ( $n$ ) = 3,  $T = 25^\circ\text{C}$ ).

The improvement in calcium removal is most dramatic as the pH increased from approximately 8 to 9.5 ( $P$  value > 0.001, making these values statistically different, given  $p = 0.05$  significance scale) and less dramatic as it was increased from 9.5 to 10.5 ( $P$  value = 0.0067). There was no

statistical difference (P value = 0.57) in the calcium removal at solution pH  $\geq 10.5$ , which approached 97%. Our data agree well with published values in the literature regarding removing calcium via pH adjustment only<sup>25,26</sup>. Calcium precipitation increased as the concentration of carbonate ions ( $\text{CO}_3^{2-}$ ) increased with increasing pH<sup>3</sup>. The ratio of  $\text{HCO}_3^-/\text{CO}_3^{2-}$  is greater than 1 at pH 7.9, approximately equal to 1 at 9.5, less than 1 at pH 10.5, and close to zero at pH 11.6. In other words  $\text{CO}_3^{2-}$  is the predominant carbonate species at pH  $\geq 10.5$ , which, therefore, is the typical pH used for calcium removal. The increasing concentration of  $\text{CO}_3^{2-}$  with increasing solution pH results in an increase in the saturation level of calcium carbonate. The Stiff and Davis index (SDI), which is a quantitative indicator of the saturation level and used to express the precipitating potential of  $\text{CaCO}_3$ , is 1.13, 2.73, 3.73, and 4.83 for pH 7.9, 9.5, 10.5, and 11.6, respectively. In addition to higher saturation, the equilibrium calcium concentration is lower for higher pH values; both impact the lower final dissolved calcium concentration at high pH seen in water softening.

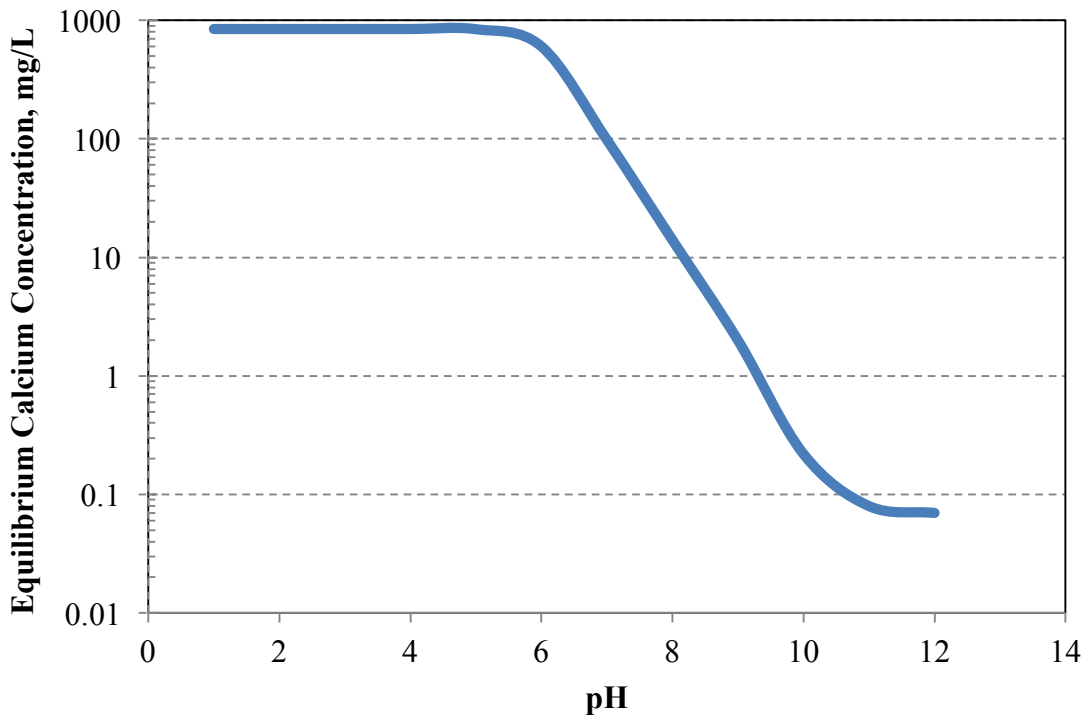


**Figure 4:** Theoretical equilibrium solubility for calcium for the synthetic water used in this experiment at various pH values. Ionic strength of fresh water was used for predictions. (T = 25 °C)

The theoretical equilibrium calcium concentration that occurs as a function of solution pH is reported in **Figure 4**. From **Figure 4** the equilibrium calcium concentration is reduced from 100 mg/L at pH 7 to  $< 1$  mg/L at pH 10.5. A previous study on precipitation softening has however demonstrated that the practical minimum solubility limit for calcium at pH 10.5 is 10 mg/L<sup>31</sup>. The difference between the theoretical and practical solubility for calcium is likely due to kinetics, competing ion effects and impacts of solution ionic strength on water activity and calcium

solubility<sup>59</sup>. Because the calcium concentrations at pH 10.5 and 11.6 were not statistically different ( $P = 0.57$ ), a solution pH of 10.5 was used in the subsequent APS experiments.

To determine the concentration of calcium carbonate seeds that provides sufficient surface area for calcium precipitation at pH 10.5, the kinetics of calcium precipitation was investigated at various seed concentrations. The change in dissolved calcium concentration as a function of reaction time for different  $\text{CaCO}_3$  seed concentrations at pH 10.5 given in **Figure 5**. The corresponding precipitation rates, *i.e.*, milligrams of precipitated calcium per minute, were determined from **Figure 5**.

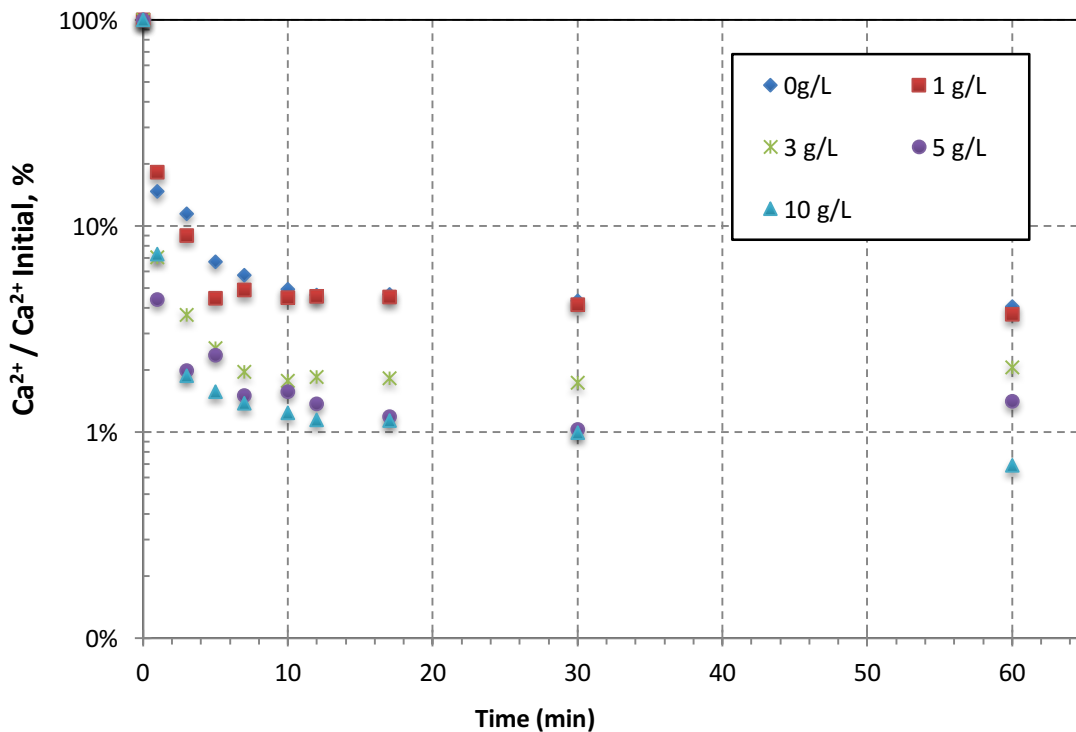


**Figure 5:** Calcium reduction for different seed concentrations using jar testing at pH = 10.5 and temperature = 25°C. Error bars are not shown for clarity. ( $n = 3$ ,  $T = 25^\circ\text{C}$ )

Precipitation kinetics were explored for seeded concentrations of 0, 1, 3, 5, and 10 g/L. The rate of calcium removal for each of the different seed concentrations was calculated for the following three time intervals: 0 to 3 mins, 3 to 10 mins, and 10 to 60 mins (**Figure 5**). The removal rate from 0 to 3 minutes differed greatly for different seeding concentrations, which leveled off after 3 minutes. Although the differences in calcium removal rates for seeded concentrations ranging from 0 g/L to 10 g/L were not quite statistically significant ( $p\text{-value} = 0.097$ ), **Figure 5** shows noticeable variations. Similar dissolved calcium reduction rates less than 250 mg  $\text{Ca}^{2+}/\text{min}$  are observed for 0, 1, and 3 g/L seeding doses. A 15% increase in rate was monitored with 5 and 10 g/L seeding doses, with calcium reduction rate up to 280 mg  $\text{Ca}^{2+}/\text{min}$ . However, higher seeding doses than 5 g/L did not result in significant additional improvement in calcium reduction rate. This suggests that 5 g/L seeding concentration generated the required surface area for nucleation, determined to be 4  $\text{m}^2/\text{L}$  of solution or 0.005  $\text{m}^2/\text{g Ca}^{2+}$ , further testing is required to understand

how the required surface area changes with starting dissolved calcium concentration<sup>56</sup>. The final calcium concentration measurement showed 96% removal ( $\text{Ca}^{2+} = 32 \text{ mg/L}$ ) for  $> 5 \text{ g/L}$  seeding and 99% removal ( $\text{Ca}^{2+} = 15 \text{ mg/L}$ ) for  $> 5 \text{ g/L}$  seeding. While the difference in calcium removal is not statistically significant ( $P = 0.19$ ), the trend shows a closer approach to the practical equilibrium calcium concentration of  $10 \text{ mg/L}$  using seeding than without seeding. A seeding concentration of  $7 \text{ g/L}$  was chosen in the following experiments to insure adequate surface area for precipitation, in addition to a reasonable reaction time. 10 minutes of reaction was chosen for further APS reaction, because less than 1% increase in calcium removal was noted after 10 minutes of reaction. Finally, it is worth pointing out that our kinetic results are consistent with literature data<sup>25,26</sup>. For example, Rahardianto et al. found that equilibrium calcium concentration was reduced to  $52 \text{ mg Ca}^{2+}/\text{L}$  after 15 minutes of reaction with seeding for PRO concentrate with a starting calcium concentration of  $740 \text{ mg/L}$  and TDS of  $7,000 \text{ mg/L}$ <sup>3</sup>.

For the following MF study, the water softening kinetics as well as optimized pH via jar testing were used. The conditions utilized were pH adjustment to 10.5,  $7 \text{ g/L}$  of calcium carbonate seed dosing, and 10 mins of softening reaction before filtration. Initially, optimization of MF conditions were carried out in dead-end filtration experiments on three different feed solutions. The untreated PRO concentrate test was used to evaluate the ability of the MF to remove calcium without softening pretreatment ('Untreated+MF'). The 'No-seeds+MF' and the 'APS+MF' tests were used to evaluate MF performance after softening without and with seeds. APS followed by 20 mins of settling without filtration was also considered ('APS+settling'). From **Figure 6** the calcium removal ranged from 0% to 99% across the different treatment types. In the absence of precipitation through either pH adjustment or APS no calcium was removed from the untreated solution by the MF ('Untreated+MF'). Recall that MF particulates and not dissolved solutes. In contrast, 'APS+MF' was the most effective treatment for removing dissolved calcium from the feed water, followed closely by 'APS+settling' and 'No-seeds+MF'. Initiating precipitation before MF as in the 'No-seeds+MF' and 'APS+MF' treatment scenarios, resulted in greater than 90% calcium removal. The 3% additional removal achieved in the 'APS+MF' treatment scheme could be attributed to the larger particles found in the APS solution compared to the 'No-seeds+MF' treatment.

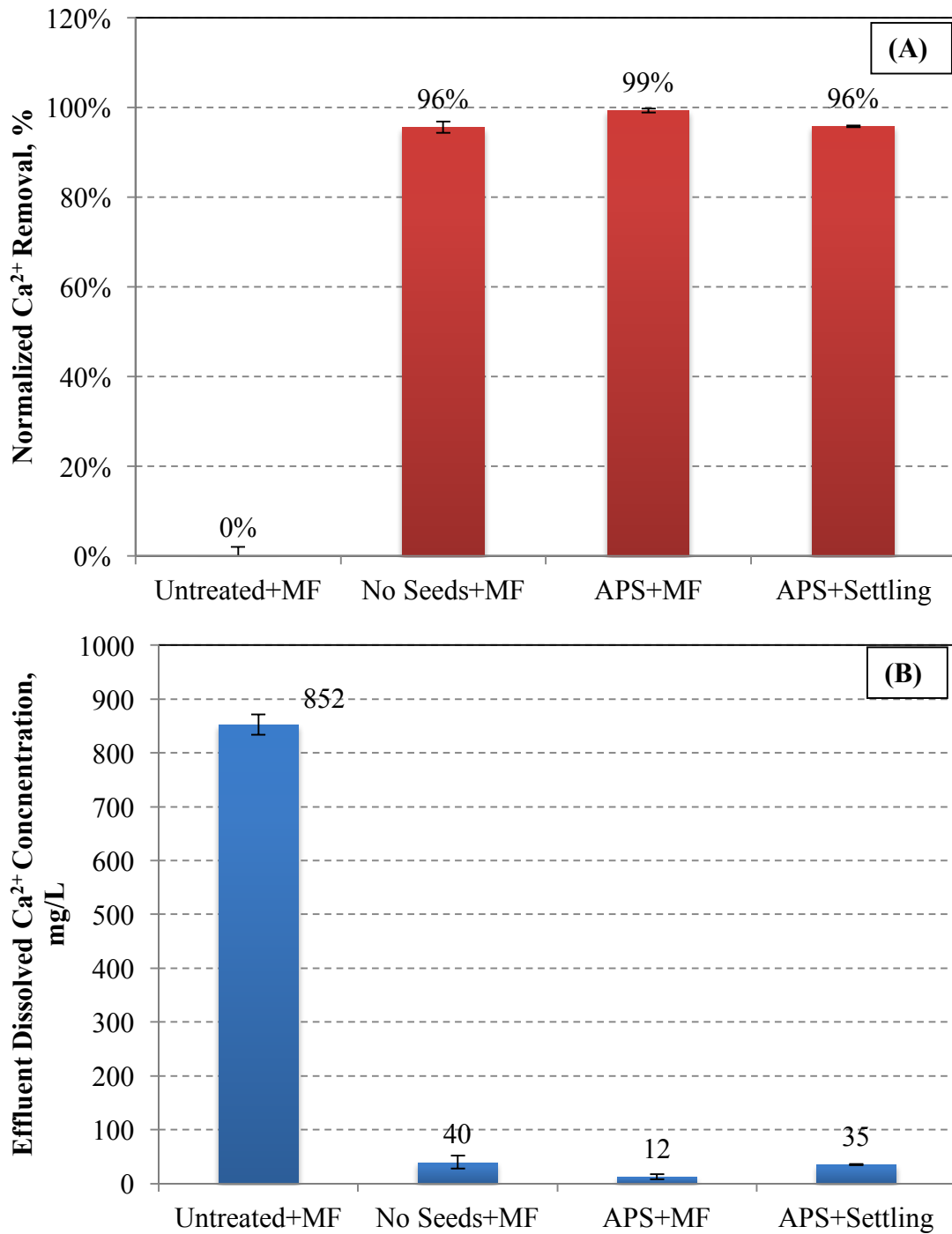


**Figure 6:** (A) Normalized calcium reduction after different levels of treatment. (B) Final dissolved calcium concentration after treatment ( $n = 3$ ,  $T = 25^{\circ}\text{C}$ ).

The small particles in the ‘No-seeds+MF’ feed may be passing through the MF membrane, resulting in a higher calcium concentration in the ‘No-seeds+MF’ effluent than in the ‘APS+MF’ effluent. This was confirmed in **Figure 7**, where the turbidity of the ‘No-seeds+MF’ effluent is much higher than the ‘APS+MF’ effluent indicating increased particulate passage.

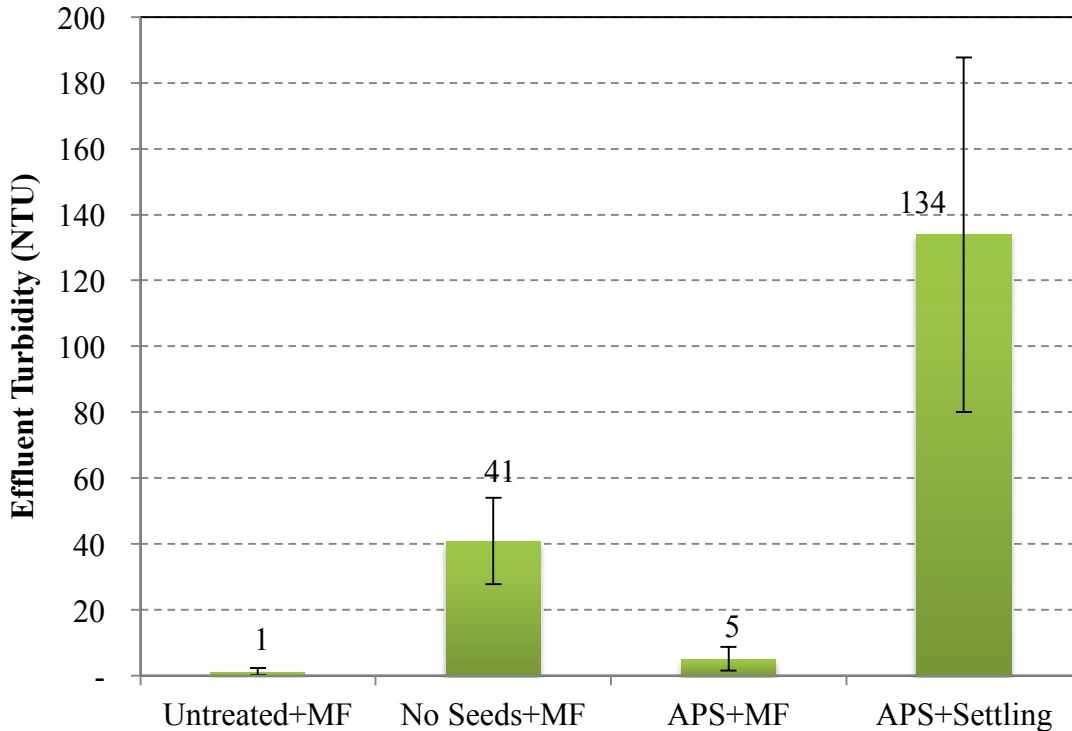
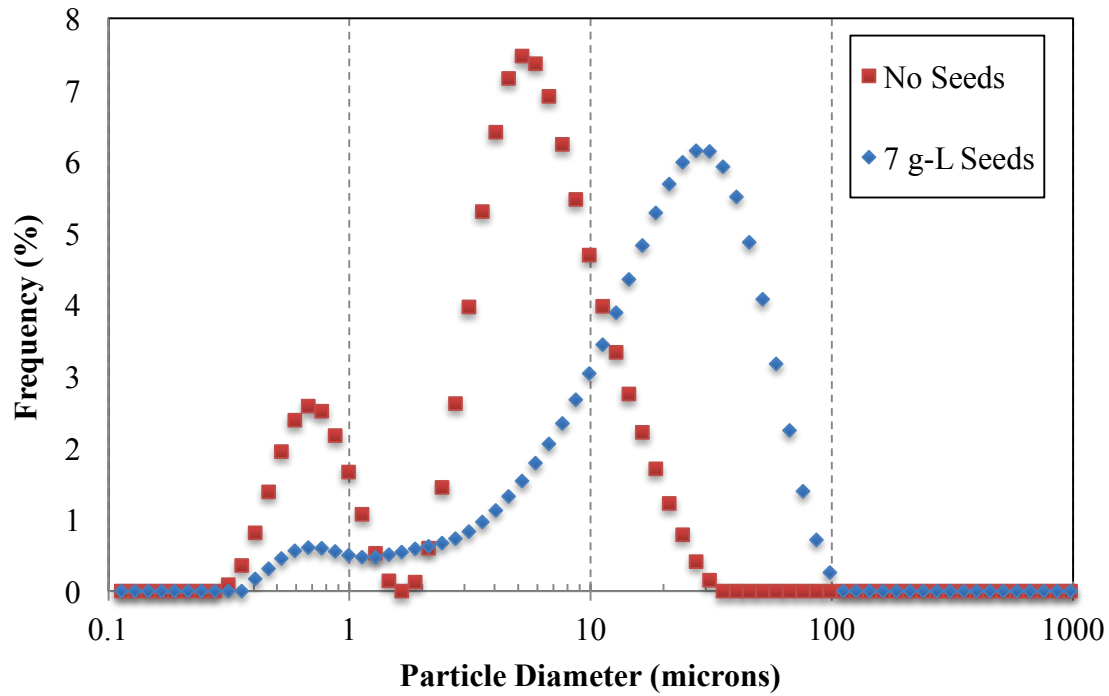


**Figure 7:** Turbidity of the effluent from different levels of treatment. The initial turbidity values for the different treatment stages were as follows: ‘Untreated+MF’ = 2.35 NTU, ‘No-seeds+MF’ = 317 NTU, and for the ‘APS+MF’ the turbidity was above the detection limit for the turbidimeter (> 800 NTU). The turbidity of the APS solution before settling was also above the detection limit the instrument ( $n = 3$ ,  $T = 25^{\circ}\text{C}$ ).

Among all the treatment scenarios, the ‘APS+MF’ treatment produced the lowest turbidity stream, generating higher quality effluent than the traditional ‘APS+settling’ treatment protocol. The ‘APS+settling’ effluent had 26× the turbidity in the ‘APS+MF’ effluent, in addition to 3% less calcium removal. To further shed light on possible particulate passage, particle size distribution in the feed was explored (**Figure 8**).



A)

B)

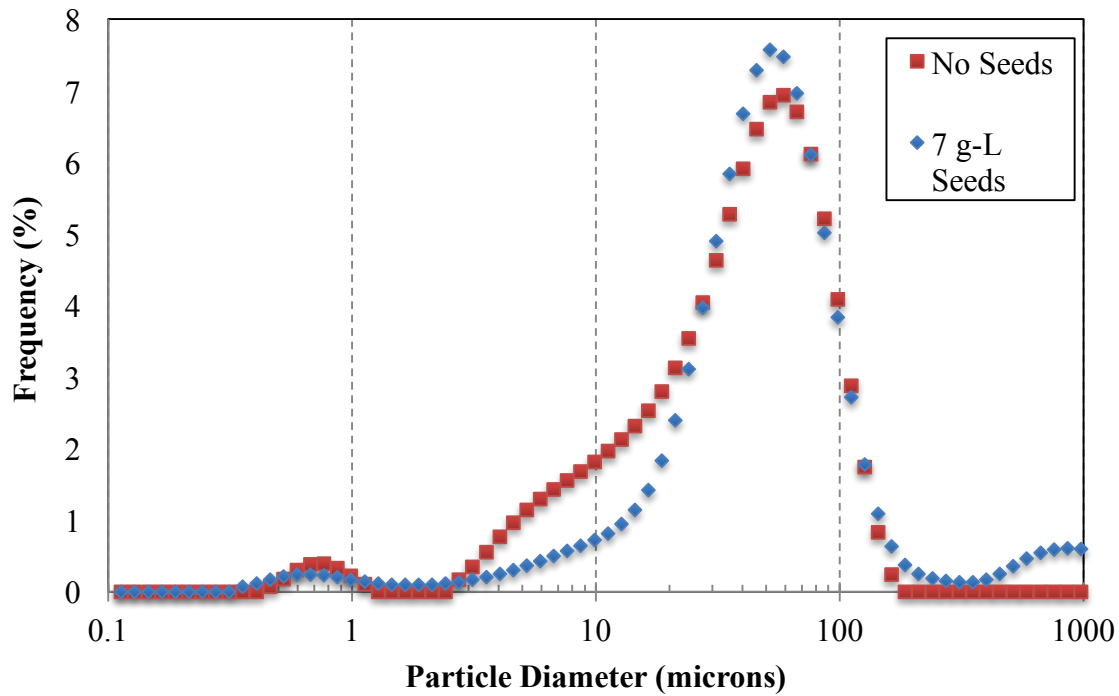


**Figure 8:** Particle size distribution measured by the granulometer after 5 (A) and 15 (B) minutes of reaction at pH 10.5

Comparing the particle size distribution among no-seeding and seeding, after 5 mins (**Figure 8a**) and 15 mins (**Figure 8b**) of the reaction, the seeded feed has its primary particle peak at 30  $\mu\text{m}$  early in the reaction and 60  $\mu\text{m}$  as the reaction proceeds. The unseeded reaction solution has peaks

at 0.67 and 6  $\mu\text{m}$  at the beginning of the reaction but they appear to grow as the reaction proceeds, with the peak shifting to 60  $\mu\text{m}$ . This indicates that the unseeded solution has particles less than 1 micron in size early in the reaction while the seeded solution has particles greater than 10 microns, this could be due to precipitate growth on the seeds in the seeded solutions rather than formation and growth of precipitates overtime in the unseeded solution. As the reaction proceeds the unseeded and seeded solutions look similar in particle size distribution, as the precipitates grow overtime in both solutions.

In addition to larger particles found in the APS feed to the MF, consequently less particle passing through the MF membrane, the formation of a cake layer may have contributed to the improved turbidity and calcium removal in the MF step, compared to the ‘no seeded+MF’ treatment. Cake layer formation with filtration of APS feed was further evidenced by the normalized water flux for the different feed conditions used for the MF membrane (**Figure 9**).

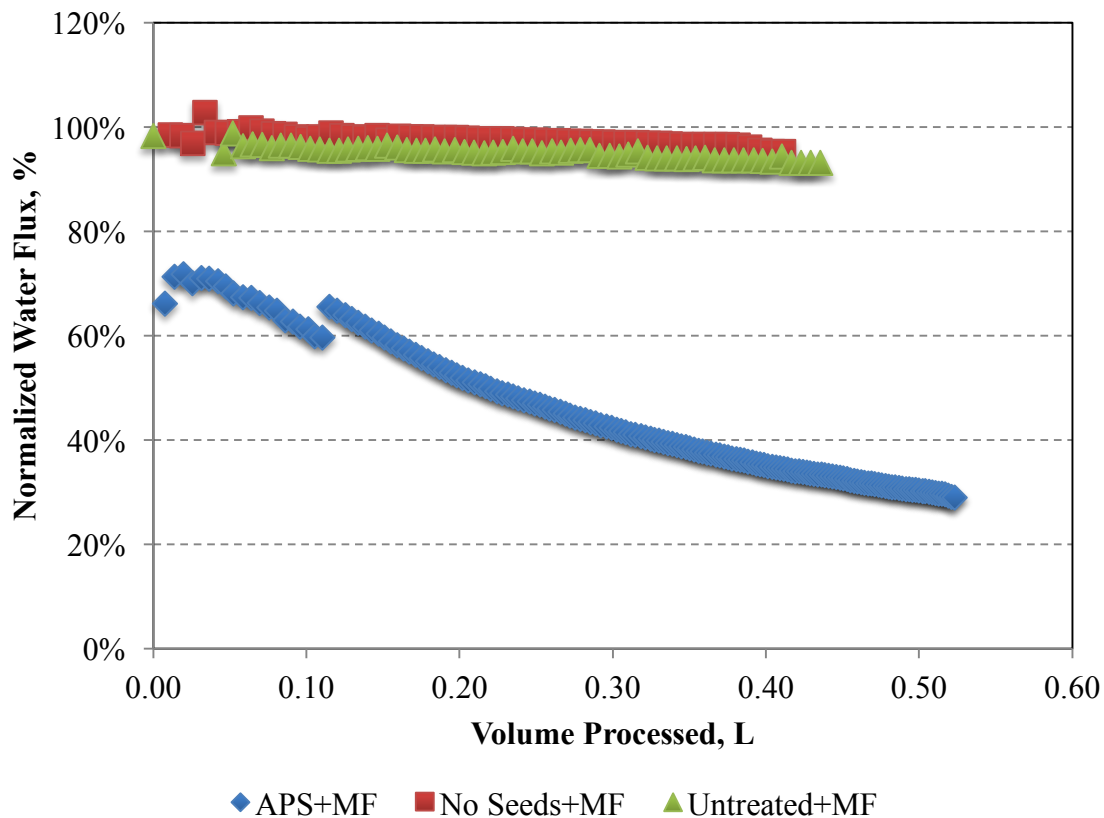


**Figure 9:** Normalized water flux as a function of the filtered water volume for the PES MF membrane with a nominal pore size of 0.45  $\mu\text{m}$  ( $P = 2 \text{ bar}$ ,  $n = 3$ ,  $T = 25^\circ\text{C}$ ).

Flux decreased by 60% from starting flux for the seeded APS treated feed water, which was possibly due to the buildup of a calcium carbonate particulate cake, from the high concentration of suspended precipitates in the feed water. Decreased flux with increasing amount of filtered water generally indicates an increase in cake thickness<sup>31</sup>. On the other hand, there was no significant flux decline for the untreated or no-seeds feed for the 500 ml of water filtered. The presence of a cake layer was confirmed by an evaluation of weight of solids remaining on the

membranes. **Table 3** shows the mass of solids loaded onto the membrane in each treatment scheme. The mass of solids was greatest for the APS feed because of the high concentration of suspended solids after the APS reaction.

**Table 3:** Mass of solids retained on the MF membrane after filtration of each feed water.

| Feed Water                     | ‘Untreated+MF’ | ‘No-seeds+MF’ | ‘APS+MF’ |
|--------------------------------|----------------|---------------|----------|
| Mass of Solids on Membrane [g] | 0.0015         | 0.005         | 0.11     |

The data reported in **Table 3** is consistent with the flux profiles reported in **Figure 9**, where the ‘APS+MF’ treatment generated 20x more solids loaded on the membrane than the ‘no-seeds +MF’ treatment, since cake build-up on the surface would cause a steady flux decline for ‘APS+MF’. The mass of solids loaded on the membrane was used to calculate the resulting cake resistance coefficient, with the cake resistance coefficient for the ‘APS+MF’ treatment shown in **Figure 10**. The cake resistance coefficient shows a steady increase in resistance to water flux due to cake build up from the calcium carbonate particulates. This is consistent with the hypothesis that cake formation was a contributor to the flux decline noted in **Figure 9**.

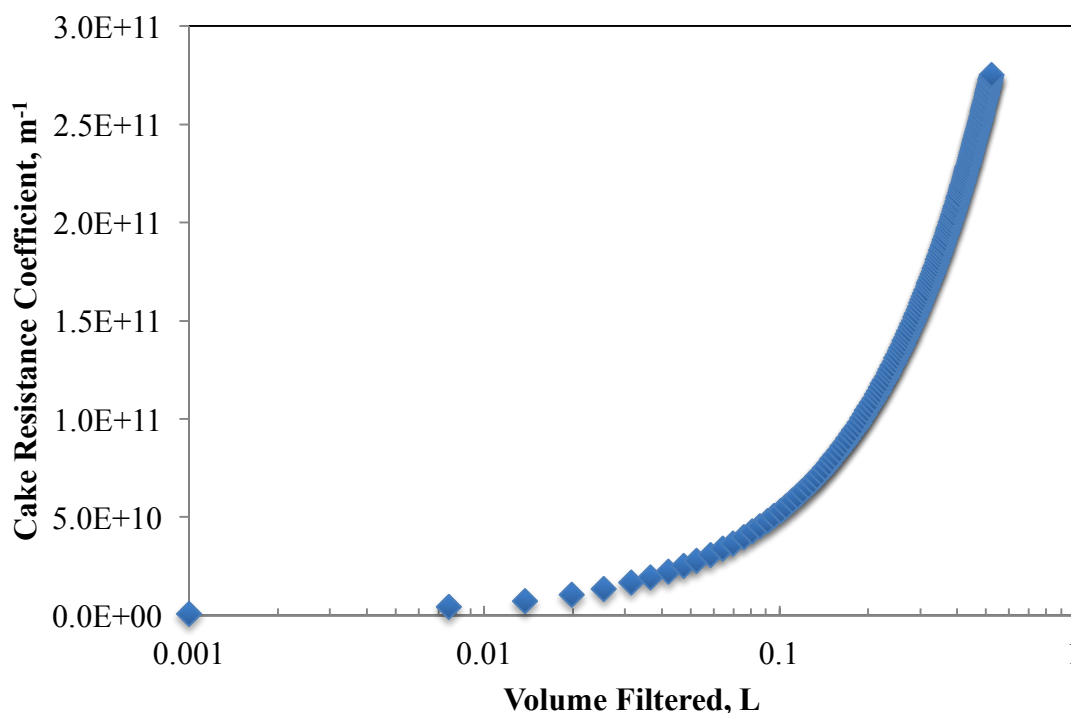


**Figure 10:** Cake resistance coefficient as a function of filtered water volume for the PES MF membrane filtering APS treated feed water. The virgin hydraulic resistance for the MF membrane was  $3.6 \times 10^{10} \text{ m}^{-1}$ .

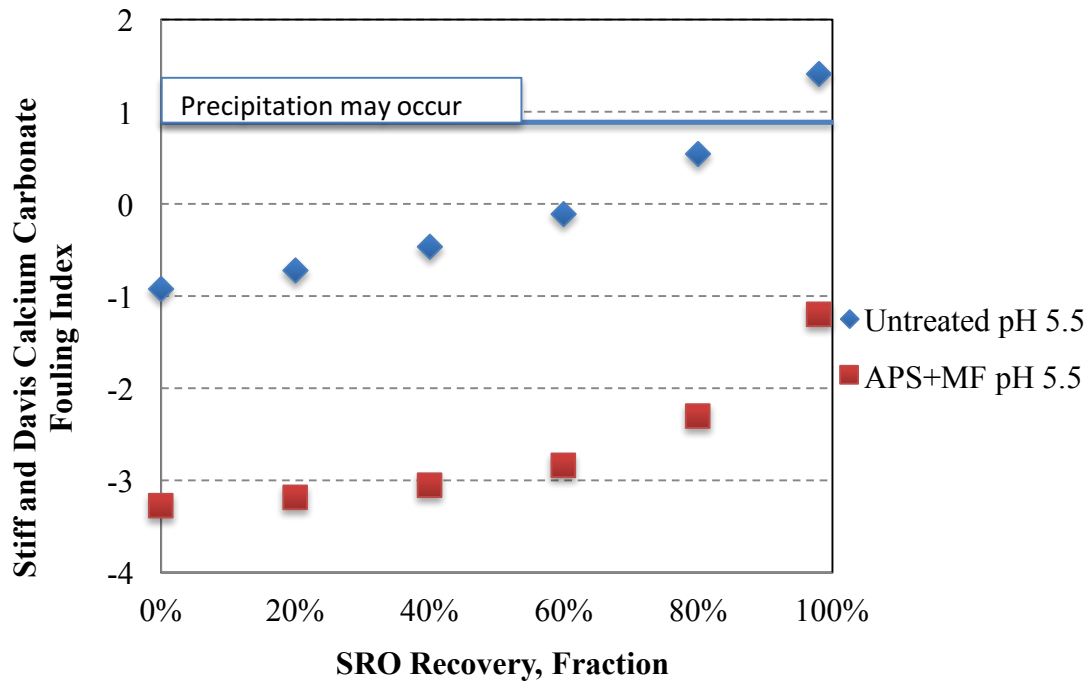
SEM/EDS analysis was done for the surface of each membrane, which showed no particles on the surface of the ‘Untreated+MF’ membrane, small groups of particles on the surface of the ‘No-

seeds+MF' membrane, and a cake layer covering the surface of the 'APS+MF' membrane. EDS analysis revealed that the particles on the surface of the membrane are primarily composed of calcium carbonate, as expected with chemical water softening. To further quantify the water quality improvement using the 'APS+MF' treatment scheme, dead-end RO testing was performed on the treated and untreated water. The fouling propensity of these water samples was evaluated by evaluating possible water recovery and SEM/EDS analysis of the surface of the membrane to explore possible fouling. The pH of both the untreated and treated RO feed solution was reduced to 5.5 using sulfuric acid to eliminate any remaining precipitates and to reduce calcium carbonate fouling tendency. The feed conditions to the dead-end RO are summarized in **Table 4**.

**Table 4:** Summary of RO feed conditions

| Feed             | Calcium Concentration (mg/L) | Turbidity (NTU) | TDS (mg/L) | pH  |
|------------------|------------------------------|-----------------|------------|-----|
| Untreated        | 852                          | 0.85            | 14,000     | 5.5 |
| 'APS+MF' Treated | 12                           | 0.1             | 14,000     | 5.5 |

The fouling propensity of the two solutions was evaluated using two RO fouling indices, *i.e.*, % saturation of calcium sulfate and the Stiff and Davis Index. If the percent saturation value of calcium sulfate reaches above 100%, it indicates fouling from calcium sulfate precipitation may occur. A Stiff and Davis Index above 1 indicates that fouling from calcium carbonate may occur. **Figure 11** shows the calcium fouling propensity for the untreated and 'APS+MF' treated feed water. With untreated feed water, both calcium carbonate and calcium sulfate fouling could occur in an RO system. While calcium carbonate fouling would not occur until 80% recovery (**Figure 11a**), calcium sulfate fouling could occur independent of recovery (**Figure 11b**). However, if the feed water was properly pretreated with the 'APS+MF' system, calcium carbonate fouling can be prevented in an RO system, as shown by **Figure 11a** ('APS+MF', pH 5.5). Additionally, calcium sulfate fouling can also be avoided, unless the water recovery rate requirement is higher than 97%.



A)

B)

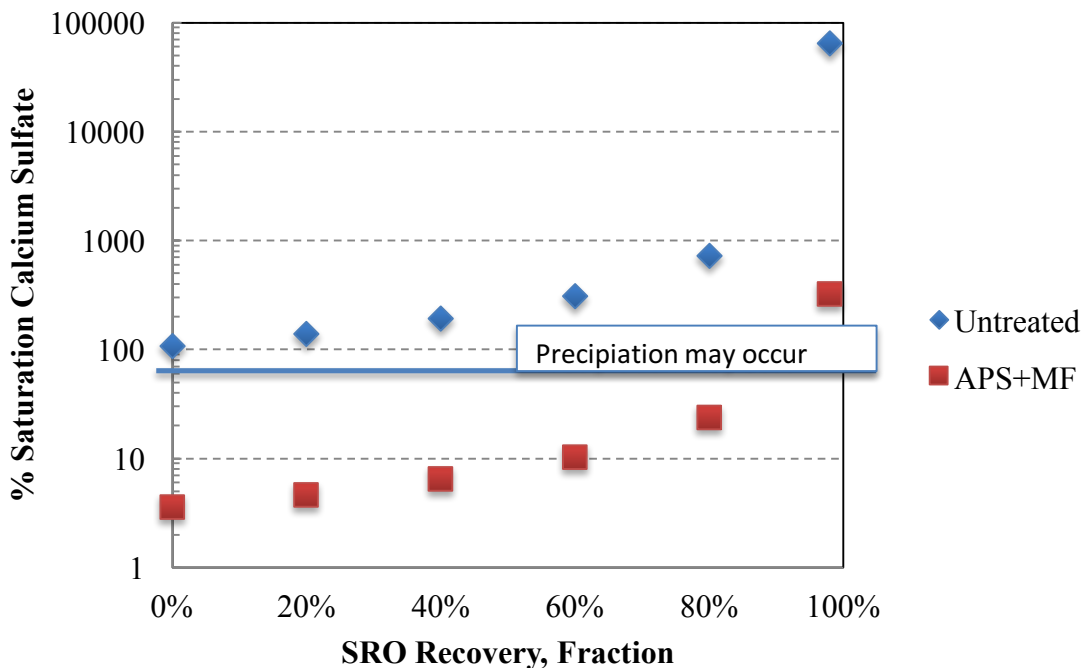


**Figure 11:** Precipitation potential during RO treatment for untreated and pretreated feed water defined by calcium fouling indices, (A) the Stiff and Davis Index and (B) % Saturation of Calcium Sulfate.

The normalized water flux as a function of the feed water recovery for the RO membrane treating the raw and APS-MF treated source water is given in **Figure 12**. For both source waters the flux declined as the recovery increased (i.e., the feed solution became more concentrated). The gradual

loss in flux can be attributed to an increase in osmotic pressure with increasing recovery. The applied pressure to the dead-end cell was not changed throughout the test, therefore as osmotic pressure increased with increasing water recovery, the water flux declined for both the treated and untreated RO tests. The theoretical change in osmotic pressure with SRO recovery is plotted in **Figure 13**.

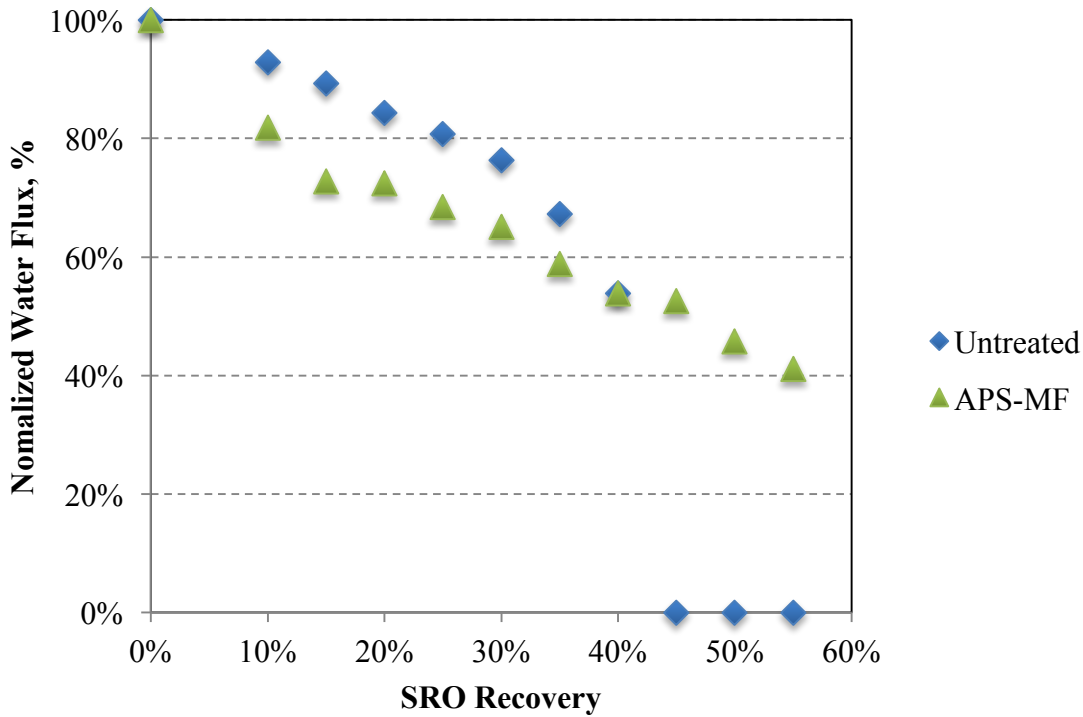


**Figure 12:** Normalized water flux vs. amount of water recovered from the system for the untreated and ‘APS+MF’ treated feed conditions. Assuming a TDS concentration of 14,000 mg/L comprised of sodium chloride and 100% RO membrane rejection ( $n = 3$ ,  $T = 25^{\circ}\text{C}$ )

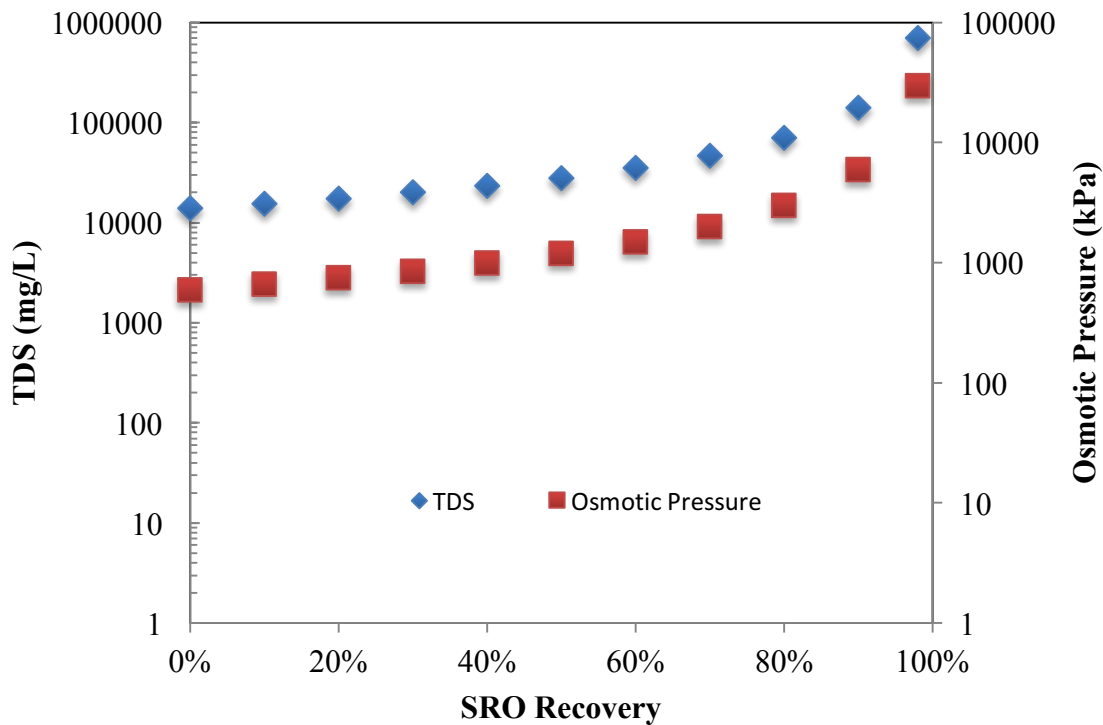


**Figure 13:** Relationship between the TDS concentration and osmotic pressure with the feed water recovery for the RO process. The initial TDS concentration was 14,000 mg/L.

**Figure 12** shows that the untreated RO test has a complete loss in flux at 40% recovery, which cannot be explained by the increase in osmotic pressure through 40% recovery seen in **Figure 13**. This could be explained using **Figure 11**, the deviation of the untreated flux from the treated flux begins at 35% SRO recovery, which corresponds with 150% calcium sulfate saturation and untreated flux stops at 40% SRO recovery, which corresponds to 200% calcium sulfate saturation. This indicates calcium sulfate scaling may have occurred on the RO membrane for the untreated feed water. FESEM analysis of the virgin and fouled RO membranes (**Figure 14**) verified the presence of mineral scale on the membrane receiving raw influent (i.e., having not been treated with the APS-MF).

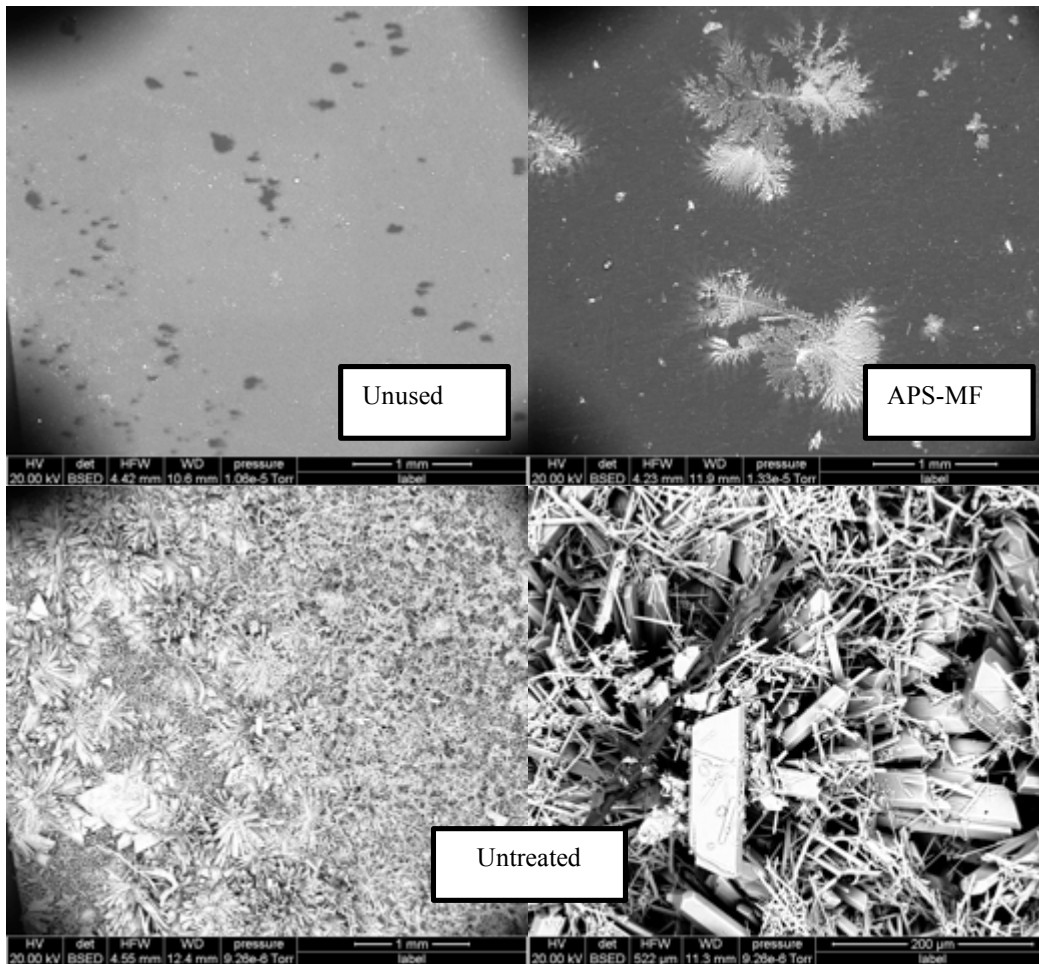


**Figure 14:** SEM images and elemental analysis of RO membranes for various feed water conditions. Surface element analysis from EDS showed 50% Calcium and 50% Sulfate for Untreated, 3% Sodium, 5% Chloride, 6% Sulfate, and >1% Calcium and Iron for APS-MF treated

From **Figure 14** the entire surface of the RO membrane for the untreated feed is covered in mineral scale crystals, consistent with the flux stoppage observed in **Figure 12**. The elemental analysis of the surface revealed that the crystals were primarily made up of calcium and sulfate, which confirmed the predictions made with data from **Figure 11**. The APS-MF treated RO test did not have any calcium scaling on the surface. Some sodium chloride crystals were observed on the surface; however, this was most likely a result of drying the membrane that had been in contact with the produced water. Therefore, the integrated APS-MF pretreatment system greatly improves the all RO system performance by treating PRO concentrate, reducing fouling in secondary RO and increasing overall water recovery.

**Integrated APS-MF System Performance.** The jar testing results from the calcium optimization studies were used to define the operating parameters for the bench scale integrated APS-MF treatment system, where both quality of the filtrate and microfiltration membrane fouling were evaluated for extended period of operation. **Figure 15** shows the visual difference in turbidity

between the feed water treated with APS and the resulting filtrate after microfiltration. It is observed that the clarity of the water is dramatically improved after the microfiltration process.



**Figure 15:** Images of the raw MF feed and its filtrate. The raw MF feed had a turbidity of  $>800$  NTU, while that for the filtrate was  $= 0.15$ NTU.

The high turbidity of the feed water ( $>800$  NTU) is due to the addition of seeds as sites for nucleation and growth of precipitates during the APS reaction, in addition to the precipitation of dissolved calcium during the APS reaction. No settling was allowed after APS, which resulted in a highly turbid feed to the MF. Total solids (TS), total suspended solids (TSS), and TDS were used to quantify the difference in water quality at different points in the process, *i.e.*, PRO concentrate as a feed, APS effluent, and filtrate after both APS and MF treatment (**Figure 16**).

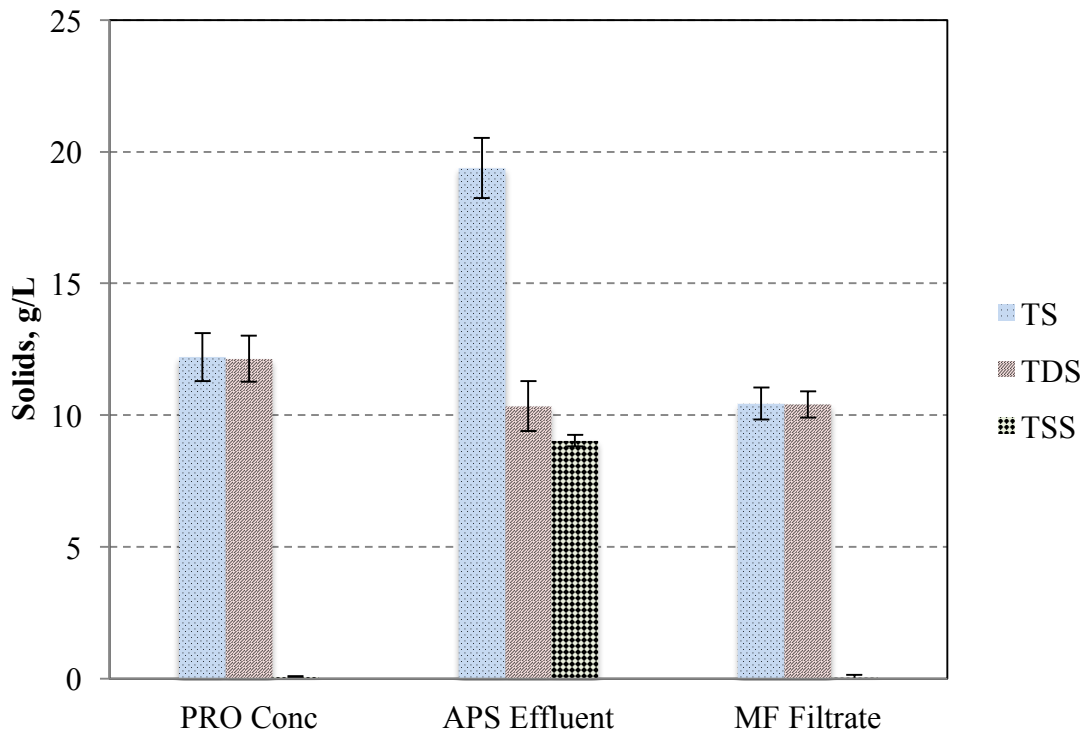


**Figure 16:** Concentrations of solids fractions in the APS effluent and MF filtrate at the beginning of the filtrate return tests. ( $n = 3$ ,  $T = 25^{\circ}\text{C}$ )

As shown in **Figure 16**, the PRO concentrate had no suspended solids, because it was a fully dissolved supersaturated solution. The APS effluent had a high concentration of suspended solids due to the introduction of seeds and the calcium precipitate totaling  $9.0 \pm 0.22$  g/L of suspended solids. There was a  $1.79 \pm 1.0$  g/L decrease in dissolved solids for the APS effluent and MF filtrate compared to the PRO concentrate, due to precipitation of dissolved calcium. At the beginning of filtrate return tests, the MF filtrate had no suspended solids, indicating that the 0.45-micron titanium dioxide ( $\text{TiO}_2$ ) MF membrane removed the majority of the suspended calcium carbonate particulates. In filtrate withdraw tests, the TSS concentration in the feed tank increased as filtrate was removed from the system (**Figure 17**). The TSS concentration remained constant throughout the operation in the filtrate return mode.

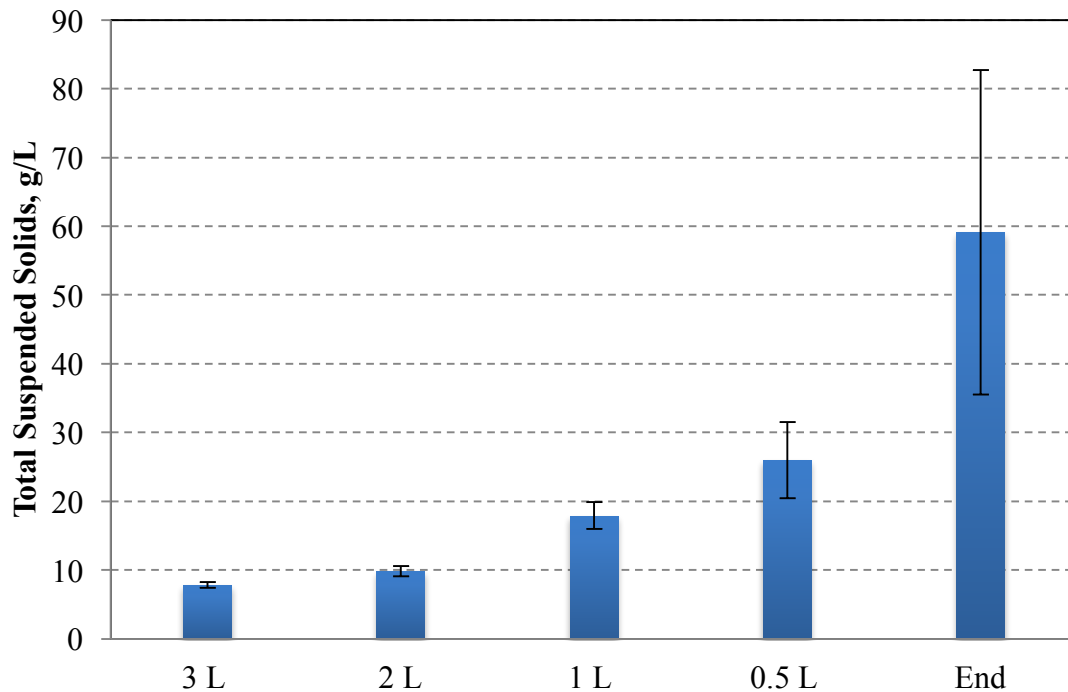
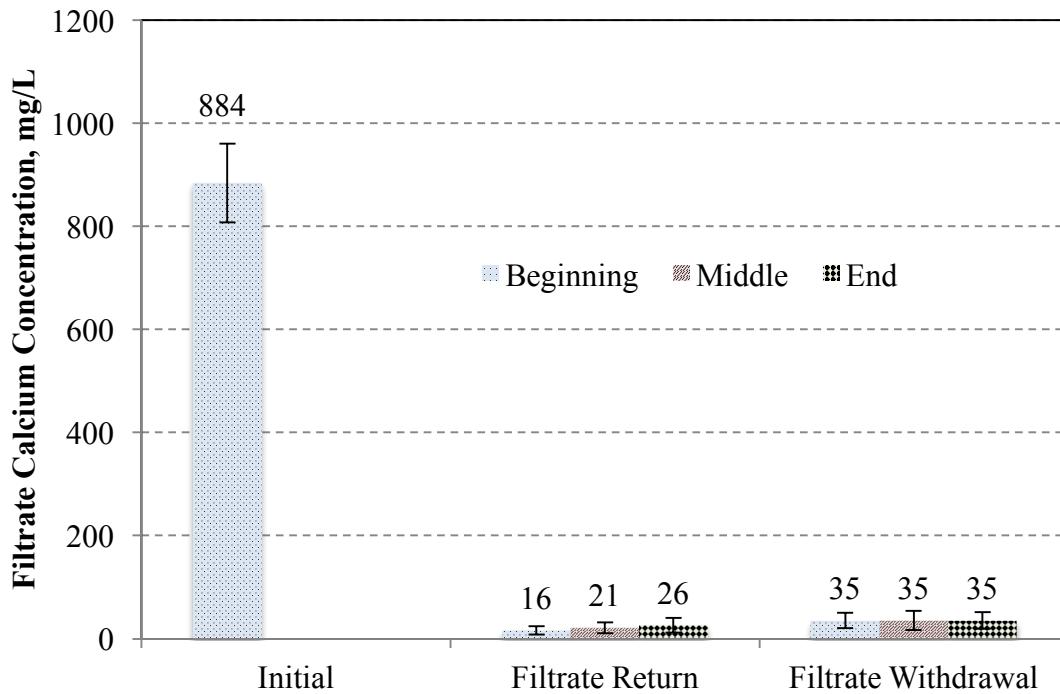


**Figure 17:** Total suspended solids during filtrate withdraw mode; feed tank is concentrated 8x the original total suspended solids by removing filtrate over time. The test was concluded when the feed tank contents could no longer be pumped through the system. ( $n = 3$ ,  $T = 25^{\circ}\text{C}$ )

With the filtrate being withdrawn from the system, the water content was lowered to 25% of the total final mass at the end of the test. Using turbidity and calcium concentration of the filtrate as indicators, the quality of the filtrate was analyzed continuously for both the filtrate return and filtrate withdraw modes to explore the possible impacts of cake filtration on water quality (**Figure 18**).



A)

B)

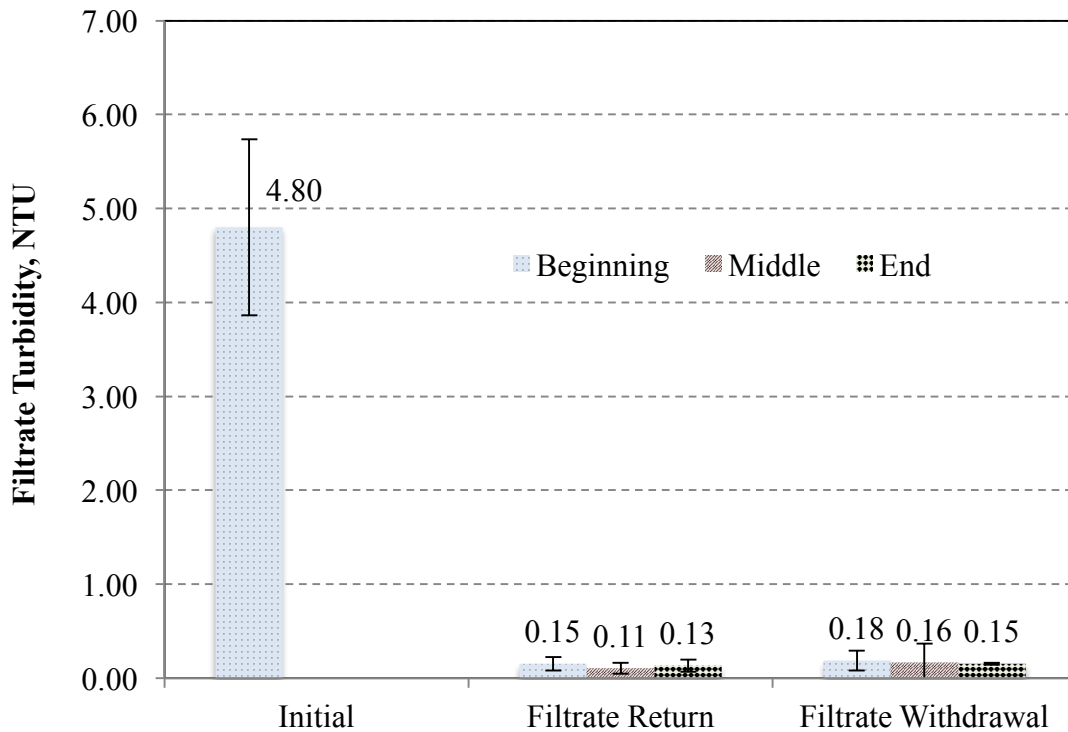
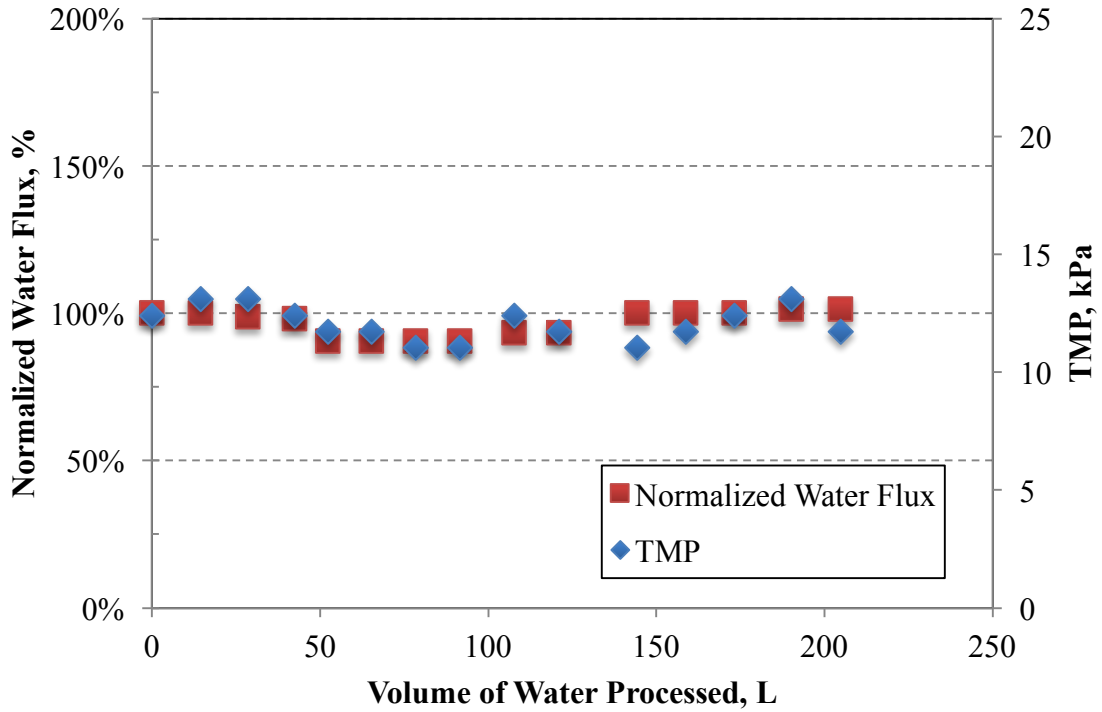


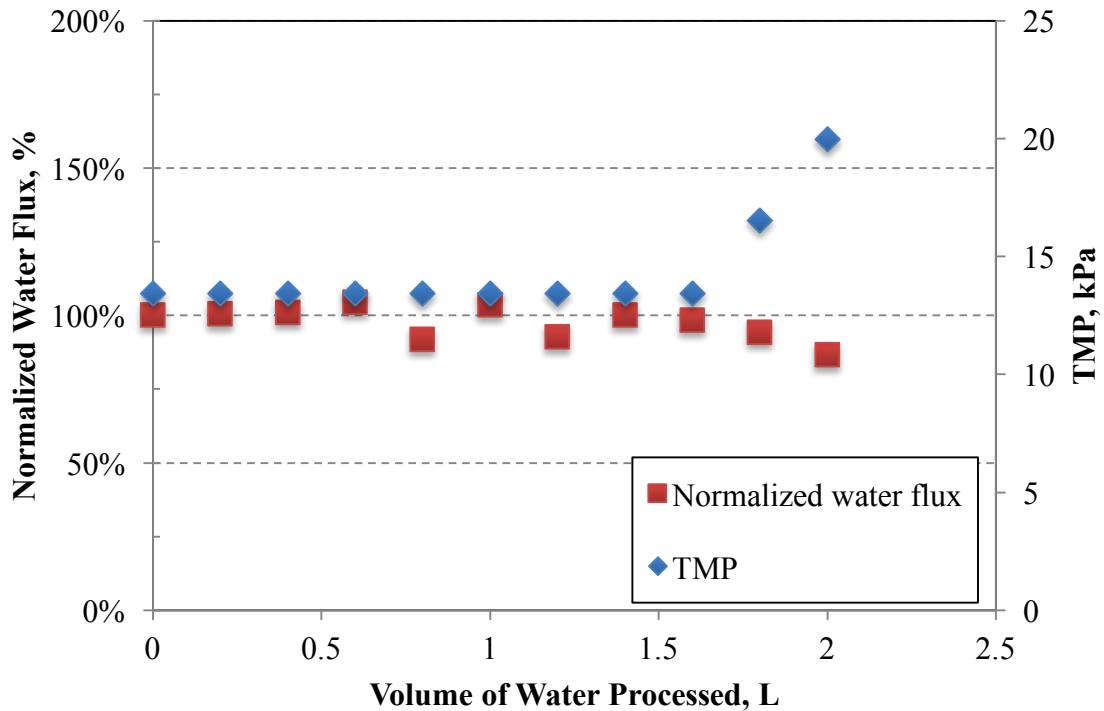
**Figure 18:** Filtrate quality for filtrate return and filtrate withdraw modes of operation. The beginning, middle, and end label refers to the averages of the water quality evaluated at the beginning, middle, and final point of overall test duration ( $n = 3$ ,  $T = 25^{\circ}\text{C}$ ).

Compared to the dead-end experimental results, where 99% reduction in dissolved calcium was achieved, the integrated APS-MF achieved a calcium reduction of 96-98%. This slightly lower calcium removal might result from the lack of cake formation on the cross-flow microfiltration membrane surface, which has been claimed to be potentially beneficial for calcium removal in some cases<sup>23,30,61</sup>. No significant decrease in calcium concentration or decrease in turbidity was observed overtime in the filtrate for either filtrate return or filtrate withdrawal mode, further indicating that cake build up did not increase over time. If a filter cake was forming or increasing overtime, filtration efficiency may improve and cause an improvement in filtrate quality (i.e., decreased calcium and turbidity). After the MF process, the turbidity was reduced below 0.5 NTU, indicating the microfiltration membrane effectively removed the suspended calcium carbonate solids. The increase in filtrate calcium concentration for the filtrate withdraw mode (96% removal, 35 mg/L Ca<sup>2+</sup>) compared to the filtrate return mode (98% removal, 21 mg/L Ca<sup>2+</sup>), could be attributed to increased calcium carbonate particulate passage, as seen by an increase in turbidity from withdraw (0.16 NTU) to return (0.13 NTU) modes. The increased particulate passage could be attributed to a higher suspended solids concentration in the filtrate withdraw feed.

Membrane fouling was explored by keeping the filtrate flux constant while monitoring TMP throughout the tests in each mode, shown in **Figure 19**. When operating the system in constant flux mode, the TMP was increased in order to maintain a constant water flux.



A)



B)

**Figure 19:** Normalized water flux and TMP for the ceramic MF membrane operated in either filtrate recycle (A) or filtrate withdraw mode (B). No backwashing was used. ( $n = 3$ ,  $T = 25^{\circ}\text{C}$ )

From **Figure 19a** there was no observed increase in TMP during operation of the cross-flow MF for filtrate return mode without the use of backwashing for 200 L of filtrate. This occurred because the ceramic MF and calcium carbonate particles are both hydrophilic therefore no “sticking” occurs between the membrane and particle. Also, cross-flow operation reduces physical build-up of particles on the MF and the use of seeded softening creates large particles that likely did not clog the membrane pores. In filtrate withdraw mode (**Figure 19b**), the TMP rose and water flux fell towards the end of the operation, most likely due to the dramatic increase in TSS observed in **Figure 17** and the significant increase in viscosity.

To confirm the successful elimination of scaling elements from the PRO concentrate, a dead-end RO experiment was performed using the cross-flow APS-MF effluent. From **Figure 20** there was a decline in flux for both the untreated and treated feed water. The gradual loss in flux can be attributed to the gradual increase in osmotic pressure with increasing recovery, while maintaining a constant applied pressure. The RO membrane used for the APS-MF treated feed was able to recover 55% of the water fed over the 12-hrs of operation. The measured 55% recovery was not the limiting recovery, it was the recovery reached during the 12-hr test. The untreated feed water completely stopped flux after only 40% water recovery.

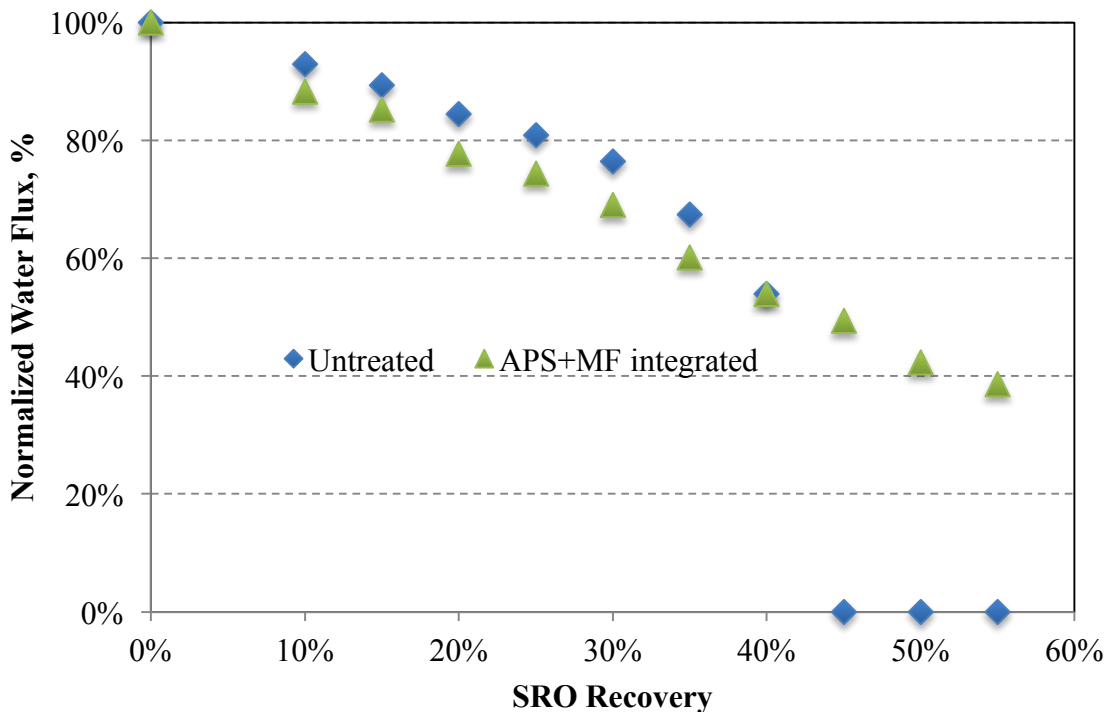


**Figure 20:** Normalized water flux as a function of the feed water recovery ratio for the RO system treating either raw or APS+MF treated feed waters.

## CONCLUSIONS

A review of produced water in Wyoming revealed that water quality varies significantly throughout Wyoming. The majority of produced waters have a high TDS concentration above

6,000 mg/L, predominately made up of sodium chloride. Produced water typically has moderate to high levels of calcium, carbonate, and sulfate. The concentration of calcium, carbonate and sulfate vary based on the location of the well. Desalination technologies must be employed to treat the produced water for reuse because of the high TDS concentration. When membrane desalination is used mineral scaling from calcium should always be considered as a possible limitation on the desalination system's water recovery. Calcium sulfate is the primary problematic mineral scalant in RO systems; because calcium carbonate scaling can be mitigated using acidification. The proposed APS-MF pretreatment scheme targets the removal of calcium to reduce calcium sulfate scaling in membrane desalination.

Our calcium removal optimization studies, for the synthetic water tested, showed that pH 10.5 and 7 g/L of seeding is the optimal pH for calcium carbonate precipitation. Dead-end MF tests in our group demonstrated that the microfiltration step effectively removed calcium carbonate precipitates produced in the softening reaction. Filtration of APS feed water produced filtrate with a 3% lower dissolved calcium concentration and 8x lower turbidity than filtrate from water softened without seeds. The improved filtrate quality is likely due to cake filtration seen in APS-MF treatment, where small precipitate particles are removed in the cake. Dead-end RO testing revealed that the untreated PRO concentrate produced mineral scaling on the RO membrane, completely stopping water flux after only 40% SRO recovery. The APS-MF treated feed water eliminated mineral scaling over the recovery range tested (up to 55% SRO recovery). SEM results confirmed that calcium sulfate scale formed on the RO membranes with untreated PRO water sample, while no calcium scaling was observed on the RO membranes with treated PRO water samples. Integrated APS-MF system performance testing data showed that APS combined with cross-flow ceramic MF system could be operated long term without significant TMP increase. In addition, it could be operated without settling the water after the APS reaction, while maintaining a reasonable operating filtrate flux and TMP. The calcium and turbidity removal seen in the integrated cross-flow APS-MF system was consistent with the dead-end tests, which also enable subsequent RO operation without noticeable calcium scaling.

**Student Support and Involvement:** We successfully graduated one Master of Science (MS) graduate student (Jennifer Hegarty) with a degree in Chemical Engineering. Two undergraduate students (Kyle Meyers, Freshman in Chemical Engineering; Weikang Li, Senior in Petroleum Engineering) were mentored by the Co-PI for 2-yrs over the project duration. All students were trained on the water chemistry and jar testing procedures for produced water analysis.

**Products:** Jennifer presented results from her research at the 2013 North American Membrane Society (NAMS) conference in Boise, ID. Her poster presentation covered her results on the characteristics of CBM produced waters, accelerated precipitation softening (optimum seed concentration for calcium removal), and RO membrane fouling in the presence/absence of the accelerated softening pretreatment. The project team has also prepared a draft manuscript on calcium removal during APS-MF treatment, with an emphasis on oil and gas produced waters. The manuscript will be submitted to the journal *Desalination* in May 2014 for publication. Finally, Jennifer successfully defended thesis in February 2014 to obtain her MS in Chemical Engineering.

## WORK CITED

1. Ebrahimi, M. *et al.* Multistage filtration process for efficient treatment of oil-field produced water using ceramic membranes. *Desalination and Water Treatment* **42**, 17–23 (2012).
2. Benko, K. L. & Drewes, J. E. Produced Water in the Western United States: Geographical Distribution, Occurrence, and Composition. *Environmental Engineering Science* **25**, 239–246 (2008).
3. Rahardianto, A., Gao, J., Gabelich, C. J., Williams, M. D. & Cohen, Y. High recovery membrane desalting of low-salinity brackish water: Integration of accelerated precipitation softening with membrane RO. *Journal of Membrane Science* **289**, 123–137 (2007).
4. Igunnu, E. T. & Chen, G. Z. Produced water treatment technologies. *International Journal of Low-Carbon Technologies* (2012). doi:10.1093/ijlct/cts049
5. Xu, P. Technical Assessment of Produced Water Treatment Technologies. *RPSEA Project* 1–158 (2009).
6. Doran, G. Developing a cost effective environmental solution for produced water and creating a new water resource. *ARCO Western Energy* 1–9 (1997).
7. Greenlee, L. F., Lawler, D. F., Freeman, B. D., Marrot, B. & Moulin, P. Reverse osmosis desalination: Water sources, technology, and today's challenges. *Water Research* **43**, 2317–2348 (2009).
8. Fakhru'l-Razi, A. *et al.* Review of technologies for oil and gas produced water treatment. *Journal of Hazardous Materials* **170**, 530–551 (2009).
9. Mondal, S. & Wickramasinghe, S. R. Produced water treatment by nanofiltration and reverse osmosis membranes. *Journal of Membrane Science* **322**, 162–170 (2008).
10. Gillespie, P. Oil and Gas Produced Water Management and Beneficial Use in the Western United States. *Science and Technology Program* **157**, 1–129 (2011).
11. Kemp, C. Bear River Basin Water Plan. *Wyoming Water Development Commission* 1–102 (2001).
12. Xu, P., Ruetten, J. & Dolnicar, S. Critical Assessment for Implementing Desalination Technology. *Water Research Foundation and Drinking Water Inspectorate* 1–230 (2009).
13. Acharya, H. Cost Effective Recovery of Low-TDS Frac Flowback Water for Re-use. *Department of Energy: DE-FE0000784* 1–100 (2011).
14. Xu, P. & Drewes, J. E. Viability of nanofiltration and ultra-low pressure reverse osmosis membranes for multi-beneficial use of methane produced water. *Separation and*

- Purification Technology* **52**, 67–76 (2006).
15. Doran, G., Williams, K. & Drago, J. Pilot Study Results to Convert Oil Field Produced Water to Drinking Water or Reuse. *Society of Petroleum Engineers* 403–417 (1998).
  16. Lawrence, A., Miller, J., Miller, D. & Hayes, T. Regional Assessment of Produced Water Treatment and Disposal Practices and Research Needs. *Society of Petroleum Engineers* 373–392 (1995).
  17. Antony, A. *et al.* Scale formation and control in high pressure membrane water treatment systems: A review. *Journal of Membrane Science* **383**, 1–16 (2011).
  18. Sheikholeslami, R. Composite scale formation and assessment by the theoretical Scaling Potential Index (SPI) proposed previously for a single salt. *Des* **278**, 259–267 (2011).
  19. Ferguson, R. & ferguson, B. The Chemistry of Strontium and Barium Scales. *Asssocation of Water Technologies* 1–17 (2010).
  20. Huang, Q. & Ma, W. A model of estimating scaling potential in reverse osmosis and nanofiltration systems. *Des* **288**, 40–46 (2012).
  21. Van der Bruggen, B., Vandecasteele, C., Van Gestel, T., Doyen, W. & Leysen, R. Review of Pressure-Driven Membrane Processes. *Environmental Progress* **22**, 43–56 (2004).
  22. Huang, H., Schwab, K. & Jacangelo, J. G. Pretreatment for Low Pressure Membranes in Water Treatment: A Review. *Environ. Sci. Technol.* **43**, 3011–3019 (2009).
  23. Oren, Y., Katz, V. & Daltrophe, N. C. Compact Accelerated Precipitation Softening (CAPS) with Submerged Filtration: Role of the CaCO<sub>3</sub> ‘Cake’ and the Slurry. *Ind. Eng. Chem. Res.* **41**, 5308–5315 (2002).
  24. Gilron, J., Daltrophe, N., Waissman, M. & Oren, Y. Comparison between Compact Accelerated Precipitation Softening (CAPS) and Conventional Pretreatment in Operation of Brackish Water Reverse Osmosis (BWRO). *Ind. Eng. Chem. Res.* **44**, 5465–5471 (2005).
  25. Qu, D. *et al.* Integration of accelerated precipitation softening with membrane distillation for high-recovery desalination of primary reverse osmosis concentrate. *Separation and Purification Technology* **67**, 21–25 (2009).
  26. Rahardianto, A., McCool, B. C. & Cohen, Y. Accelerated desupersaturation of reverse osmosis concentrate by chemically-enhanced seeded precipitation. *Des* **264**, 256–267 (2010).
  27. Rahardianto, A., Gao, J., Gabelich, C. J., Williams, M. D. & Cohen, Y. High recovery membrane desalting of low-salinity brackish water: Integration of accelerated precipitation softening with membrane RO. *Journal of Membrane Science* **289**, 123–137

- (2007).
28. Zhong, J., Sun, X. & Wang, C. Treatment of oily wastewater produced from refinery processes using flocculation and ceramic membrane filtration. *Separation and Purification Technology* **32**, 93–98 (2003).
  29. Rajagopalan, N. Field Evaluation of Ceramic Microfiltration Membranes in Drinking Water Treatment. *Montana University System Water Center* 1–4 (2001).
  30. Kedem, O. & Zalmon, G. Compact accelerated precipitation softening (CAPS) as a pretreatment for membrane desalinationI. Softening by NaOH. *Desalination* **113**, 65–71 (1997).
  31. Crittenden, J. C., Trussell, R. R., Hand, D. H., Howe, K. J. & Tchobanoglous, G. *Water Treatment: Principles and Design*. (John Wiley Sons, INC, 2005).
  32. International Energy Outlook 2013 - Energy Information Administration. *eia.gov* (2014). at <<http://www.eia.gov/forecasts/ieo/index.cfm>>
  33. Azetsu-Scott, K. *et al.* Precipitation of heavy metals in produced water: Influence on contaminant transport and toxicity. *Marine Environmental Research* **63**, 146–167 (2007).
  34. Survey, U. S. G. USGS Produced Water Database. (2006). at <<http://energy.cr.usgs.gov/prov/prodwat/data.htm>>
  35. Benko, K. L. & Drewes, J. E. Produced Water in the Western United States: Geographical Distribution, Occurrence, and Composition. *Environmental Engineering Science* **25**, 239–246 (2008).
  36. Koutsoukos, P. Common Foulants in Desalination: Inorganic Salts. *Encyclopedia of Desalination and Water Resource* 1–17 (2012).
  37. Shirazi, S., Lin, C.-J. & Chen, D. Inorganic fouling of pressure-driven membrane processes — A critical review. *Des* **250**, 236–248 (2010).
  38. Guo, W., Ngo, H.-H. & Li, J. A mini-review on membrane fouling. *Bioresource Technology* **122**, 27–34 (2012).
  39. McCool, B. C., Rahardianto, A. & Cohen, Y. Antiscalant removal in accelerated desupersaturation of RO concentrate via chemically-enhanced seeded precipitation (CESP). *Water Research* **46**, 4261–4271 (2012).
  40. Ferguson, R., ferguson, B. & Stancavage, R. Modeling Scale Formation and Optimizing Scale Inhibitor Dosages in Membrane Systems. *AWWA Membrane Technology Conference* 1–19 (2011).
  41. Chesters, S. & Armstrong, M. Cost saving case study using a calcium sulphate specific antiscalant. *IDA World Congress* 1–10 (2009).

42. Ferguson, R. Mineral Scale Prediction and Control at Extreme TDS. 1–12 (2011).
43. Huang, H., Cho, H.-H., Schwab, K. J. & Jacangelo, J. G. Effects of magnetic ion exchange pretreatment on low pressure membrane filtration of natural surface water. *Water Research* **46**, 5483–5490 (2012).
44. Xu, P. & Drewes, J. E. Viability of nanofiltration and ultra-low pressure reverse osmosis membranes for multi-beneficial use of methane produced water. *Separation and Purification Technology* **52**, 67–76 (2006).
45. Waly, T., Kennedy, M. D., Witkamp, G.-J., Amy, G. & Schippers, J. C. The role of inorganic ions in the calcium carbonate scaling of seawater reverse osmosis systems. *Des* **284**, 279–287 (2012).
46. Waly, T., Kennedy, M. D., Witkamp, G.-J., Amy, G. & Schippers, J. C. Will calcium carbonate really scale in seawater reverse osmosis? *Desalination and Water Treatment* **5**, 146–152 (2009).
47. Lower, S. Carbonate equilibria in natural waters. *Environmental Chemistry* **Chem1**, 1–26 (1999).
48. Nason, J. A. & Lawler, D. F. Particle size distribution dynamics during precipitative softening: Constant solution composition. *Water Research* **42**, 3667–3676 (2008).
49. Szwarc, M. ‘Living’ Polymers. *Nature* **178**, 1168–1169 (1956).
50. CUI, Z., PENG, W., FAN, Y., XING, W. & XU, N. Effect of Cross-flow Velocity on the Critical Flux of Ceramic Membrane Filtration as a Pre-treatment for Seawater Desalination. *Chinese Journal of Chemical Engineering* **21**, 341–347 (2013).
51. Ould-Dris, A., Jaffrin, M. Y., Si-Hassen, D. & Neggaz, Y. Analysis of cake build-up and removal in cross-flow microfiltration of CaCO<sub>3</sub>. *Journal of Membrane Science* **175**, 267–283 (2000).
52. Yildiz, E., Nuhoglu, A., Keskinler, B., Akay, G. & Farizoglu, B. Water softening in a crossflow membrane reactor. *Desalination* **159**, 139–152 (2003).
53. Kweon, J. H. & Lawler, D. F. Fouling mechanisms in the integrated system with softening and ultrafiltration. *Water Research* **38**, 4164–4172 (2004).
54. Afonso, M., Alves, A. & Mohsen, M. Crossflow microfiltration of marble processing wastewaters. *Desalination* **149**, 153–162 (2002).
55. Ould-Dris, A., Jaffrin, M. Y., Si-Hassen, D. & Neggaz, Y. Effect of cake thickness and particle polydispersity on prediction of permeate flux in microfiltration of particulate suspensions by a hydrodynamic diffusion model. *Journal of Membrane Science* **164**, 211–227 (2000).

56. Sukhorukov, G. B. *et al.* Porous calcium carbonate microparticles as templates for encapsulation of bioactive compounds. *J. Mater. Chem.* **14**, 2073 (2004).
57. Doll, J. M. & Foster, J. C. The Effect of Calcium Carbonate Particle Size and Shape on the Properties and Performance of Calcium Carbonate Granulations. *Specialty Minerals Inc* 1–21 (2009).
58. Khean, T. Studies in Filter Cake Characterization and Modelling. *University of Malaya* 1–194 (2003).
59. Coto, B., Martos, C., Peña, J. L., Rodríguez, R. & Pastor, G. Effects in the solubility of CaCO<sub>3</sub>: Experimental study and model description. *Fluid Phase Equilibria* **324**, 1–7 (2012).
60. Gilron, J., Chaikin, D. & Daltrophe, N. Demonstration of CAPS pretreatment of surface water for RO. *Desalination* **127**, 271–282 (2000).
61. Oren, Y., Katz, V. & Daltrophe, N. Improved Compact Accelerated Precipitation Softening (CAPS). *Desalination* **139**, 155–159 (2001).